



Tonkin & Taylor

Liquefaction Vulnerability Study

ENVIRONMENTAL AND ENGINEERING CONSULTANTS



REPORT

Earthquake Commission

Liquefaction vulnerability study

It is intended that this report and the accompanying datasets will be re-issued in the future to reflect the expansion of geotechnical datasets that are being obtained as part of the Canterbury reconstruction

Report prepared for:
EARTHQUAKE COMMISSION

Report prepared by:
Tonkin & Taylor Ltd

Distribution:
Earthquake Commission
Tonkin & Taylor Ltd (FILE)

1 copy + digital

1 copy

February 2013

T&T Ref: 52020.0200/v1.0



Executive Summary

The Canterbury area has been affected by a large number of earthquakes following the initial earthquake on 04 September 2010. These earthquakes have been observed to cause widespread liquefaction, lateral spreading and ground surface subsidence. In parts of Canterbury, the liquefaction and lateral spreading caused extensive damage to residential land, dwellings and infrastructure. In some areas of Christchurch there was only minor liquefaction related damage observed and in other areas there was no observed damage at the ground surface even though liquefaction of some of the underlying soil layers most likely occurred. The reasons why some areas of land susceptible to liquefaction performed better than other areas are not well defined in liquefaction publications.

The New Zealand Government have classified land in Canterbury into various categories as a result of the recent earthquake series. The residential Red Zone is land identified by the Government as unsuitable for occupation at the present time. For the balance of the land (classified residential Green Zone), the Ministry of Building, Innovation and Employment (MBIE) developed technical categories to assist with the residential recovery process. Residential Red Zone areas generally encompass the most severely damaged land in Canterbury. TC2 and TC3 areas have been identified as locations where liquefaction damage is possible in a future large earthquake. TC3 areas require site specific investigation and foundation design. TC2 areas have acceptable foundation solutions specified.

The unprecedented liquefaction related land and dwelling damage during the recent earthquake series in Canterbury has highlighted the need to better understand the vulnerability of land to liquefaction damage caused by future earthquakes. This report summarises a review of liquefaction vulnerability parameters used to predict liquefaction damage and to assess how they compare with the observed damage. The objectives of the study were to either confirm the suitability of an existing published method or develop a new liquefaction vulnerability parameter that is suitable for both predicting the future vulnerability and also measuring the change in vulnerability that has occurred as a result of the earthquakes in Canterbury.

Visual observations of the land damage and dwelling foundation damage mapping over Canterbury show that the majority of areas most severely affected by liquefaction coincide with low lying areas where the ground water table is shallow. Conversely, sites less affected by liquefaction are in areas of higher elevation where the depth to ground water is low, indicating there is some correlation between liquefaction damage and the non-liquefying crust thickness. Analyses show that even though there is a lot of scatter, the likelihood of liquefaction related damage increases with decreasing crust thickness. The scatter is attributed to other variables that also control land performance.

A geotechnical investigation comprising more than 7,000 cone penetration tests, 1,000 boreholes and laboratory testing was supplemented by a groundwater investigation comprising more than 800 monitoring wells. These datasets are used in this report to characterise land vulnerability to the liquefaction hazard by comparing the existing published liquefaction vulnerability assessment tools of Liquefaction Potential Index (LPI), calculated settlement indicator from predictive correlations (S) and a new parameter developed by Tonkin & Taylor, the Liquefaction Severity Number (LSN). The various parameters represent liquefaction vulnerability and include crust thickness, varying soil conditions, shaking intensity, shaking duration and groundwater levels. The current MBIE (2012) guidance uses a calculated settlement indicator to assess land performance for foundation design purposes.

The analyses show that LPI produces correlations with clear trends within each earthquake damage dataset, but that the trends vary between earthquakes. This limits the usefulness of LPI as a predictive tool as the index ranges indicating damage vary depending on the magnitude and location of the earthquakes that may occur. It is also noted that the calculated range of LPI values for each of the mapped land and dwelling damage categories is not consistent with the published indicators of damage category.

The analyses undertaken show there is no apparent relationship between the calculated settlement indicator (S) and the measured liquefaction induced ground surface subsidence. This is because ground surface subsidence could be affected by the ejection of liquefied material, lateral spread and repeated liquefaction (mechanisms which are not included in the calculated settlement method). However, there is a correlation between the calculated settlement indicator and the earthquake damage datasets. Therefore, the calculated settlement can be considered as a proxy for predicting the likelihood of liquefaction related damage. While calculated settlement shows a clear trend of differentiating residential Red Zone properties from others, there is a significant amount of overlap in the damage severity mapped at residential properties.

The LSN parameter refines the calculated settlement parameter by including a depth weighting function. The depth weighting function recognises that ground surface damage from shallow liquefied layers is more likely than from deeper layers. The LSN analyses show that there is a consistent correlation with the earthquake damage dataset, both within each earthquake and between various earthquakes for the different categories of liquefaction and lateral spreading observations. The LSN clearly differentiates the most severely damaged land from the least affected land.

Of the three *calculated parameters* considered, LSN is the most suitable tool for predicting future land performance in Canterbury and provides the best correlations with the observations made in Canterbury. LSN is a good indicator of liquefaction vulnerability for residential land that is flat and confined. LSN is not intended as an indicator of vulnerability to lateral spreading hazard. Therefore, in order to identify land that is prone to liquefaction related ground surface deformation, areas identified as having lateral spreading hazard must also be considered although this falls outside the scope of this study.

The prediction of liquefaction damage from potential future earthquakes shows that land in the residential Red Zone is vulnerable at low levels of seismic load (i.e. under short return period earthquakes) and has the greatest vulnerability at higher levels of seismic load. Land in TC2 and TC3 areas is considerably less vulnerable than residential Red Zone land. The findings of this study can also be applied to areas beyond Canterbury, but consideration will need to be given to the different soil conditions in other areas that may not perform in the same way.

Table of contents

Executive summary

Glossary	1
1 Introduction	5
1.1 Objectives	5
1.2 Outline	5
1.3 Applicability	7
2 Background	8
2.1 Canterbury earthquakes and liquefaction	8
2.2 Regulatory framework	9
3 Field investigations and damage mapping	10
3.1 General	10
3.2 Mapped land and dwelling foundation damage attributes	10
3.2.1 Mapped land damage attributes	10
3.2.2 Mapped dwelling foundation damage attributes	11
3.2.3 Residential Red Zone	12
3.3 Correlation between land and dwelling foundation damage attributes	12
3.4 Seismic loading	12
3.5 Survey and regional deformation	13
3.6 Other mapping	16
3.7 Geotechnical investigations	17
3.8 Groundwater design models	17
3.9 Damage attribute summary	19
4 Liquefaction triggering	19
4.1 General	19
4.2 Idriss & Boulanger	19
4.3 Ic-based liquefaction potential	20
4.4 Soil density	20
4.5 Thin layer correction	21
4.6 Comparison of CPT and SPT-based liquefaction triggering	21
4.7 Pre-digging of CPT locations	21
5 Published liquefaction vulnerability indicators	22
5.1 General	22
5.2 Literature review	22
5.3 Comparison of damage attributes with Ishihara criteria	23
6 Calculated parameters	24
6.1 General	24
6.2 Liquefaction Potential Index (LPI)	24
6.3 Calculated settlement indicator (S)	24
6.4 Liquefaction Severity Number (LSN)	24
7 Sample CPT and response to PGA	25
8 Datasets and interpolation	27
8.1 General	27
8.2 Dataset development	27
8.3 Damage attribute quality	28
9 Damage attribute and calculated parameter comparison	29
9.1 General	29

9.2	Scatter in datasets	30
9.3	Primary dataset results	32
9.3.1	General	32
9.3.2	Liquefaction Potential Index (LPI)	32
9.3.3	Calculated settlement indicator (S)	33
9.3.4	Liquefaction Severity Number (LSN)	34
9.3.5	Maps	34
9.4	Conclusions	35
10	Study of additional earthquakes	36
10.1	General	36
10.2	Earthquake comparison – 16 April 2011	37
10.3	Earthquake comparison – 13 June 2011 (Event A)	37
10.4	Earthquake comparison – 23 December 2011 (Event A and B combined)	37
11	Future performance	38
11.1	General	38
11.2	Primary dataset analysis	38
11.2.1	Inputs	38
11.2.2	Results	39
11.3	Observed liquefaction at 100 year return period seismic loading	40
11.4	Sensitivity to groundwater	40
12	LSN and lateral spread	41
13	Examples of LSN	42
14	Discussion	43
15	Summary and conclusions	47
16	Acknowledgements	50
	References	i

Appendix A:	Figures
Appendix B:	CPT Liquefaction triggering method and multiple earthquake modelling
Appendix C:	Groundwater modelling methodology
Appendix D:	Individual CPT analyses
Appendix E:	Interpolation
Appendix F:	Earthquakes - maps
Appendix G:	Main earthquakes - graphs and analysis
Appendix H:	Calculated settlement indicator maps
Appendix I:	LSN Maps
Appendix J:	Calculated settlement indicator and LSN graphs
Appendix K:	Observed Liquefaction performance at approximately 100 year PGA
Appendix L:	Groundwater sensitivity
Appendix M:	Avonside study area – lateral spreading
Appendix N:	LSN Examples

Glossary

Term	Definition
100 year event 1 in 100 AEP	Shorthand for the earthquake with a 1 in 100 (1%) annual exceedance probability (AEP). In urban Christchurch under the current seismic models, this is broadly equivalent to the shaking intensity experienced in urban Christchurch in the 04 September 2010 earthquake. This is modelled as a 0.2g, M7.5 earthquake load.
Calculated parameter	An indicator of liquefaction vulnerability. Typically calculated based on CPT results for different scenarios. An example of a <i>calculated parameter</i> is the cumulative thickness of liquefied material in a specific earthquake using a specific liquefaction triggering method.
CERA	Canterbury Earthquake Recovery Authority. Agency established by the Government to lead and coordinate the ongoing recovery effort following the earthquakes.
CGD Canterbury Geotechnical Database	A public database of geotechnical data for the Canterbury region and used in this analysis. Located at https://canterburygeotechnicaldatabase.projectorbit.com/
CPT Cone Penetration Test	Geotechnical ground investigation test pushing an instrumented cone into the ground at a controlled rate and measuring the tip resistance, sleeve friction and dynamic pore water pressure.
CPT triggering (simplified method)	Method used to assess the likelihood of a given soil layer liquefying under seismic loading. Compares the cyclic resistance ratio (CRR) to the cyclic stress ratio (CSR) and calculates a factor of safety against liquefaction for a given situation.
CRR Cyclic Resistance Ratio	A representation of the ability of the ground to resist liquefaction.
CSR Cyclic Stress Ratio	A representation of the liquefaction demand imposed on the ground by seismic shaking.
CT Crust Thickness	The thickness of the uppermost layer of non-liquefying material.
CTL Cumulative Thickness of Liquefaction	The total thickness of liquefaction that was calculated to have occurred over the CPT trace.

Damage attributes	Measured damage indicators, typically comprising residential land damage, liquefaction induced dwelling foundation damage and liquefaction induced elevation change. The measured <i>damage attributes</i> are compared with the <i>calculated parameters</i> to determine the best fit.
DEM Digital Elevation Model	A digital ground surface elevation model derived from the LiDAR survey points.
Dwelling damage or dwelling foundation damage	The damage caused to a dwelling foundation by liquefaction, comprising stretching, hogging, dishing, racking/twisting, tilting, discontinuous foundation or global settlement.
EQC Earthquake Commission	The Earthquake Commission who administer the Earthquake Commission Act 1993.
Fines content	The proportion of fine grained material present in the soil. Typically defined as silt and clay sized particles passing the 63 micron sieve.
FoS Factor of safety against liquefaction	The ratio of CRR/CSR. FoS of 1.0 or more indicates no liquefaction (i.e. capacity exceeds demand). FoS less than 1.0 indicates liquefaction is likely (i.e. demand exceeds capacity).
GeoNet	The network of seismometers in New Zealand operated by GNS.
GNS	GNS Science (formerly Institute of Geological and Nuclear Sciences) is a crown research institute in New Zealand and operate the seismic recording stations (GeoNet) and carry out seismicity modelling.
Groundwater depth	The depth from the ground surface to the water table.
H1, H2	Ishihara's (1985) notation for the thickness of a non liquefying crust (H1) and the thickness of the liquefied layer beneath this (H2).
I&B or IB Idriss & Boulanger	Method for assessing CPT triggering CRR and CSR.
Ic Soil behaviour type index	A single value calculated from the CPT data for each soil layer that represents the normalised cone parameters (i.e. whether the soil behaves as a coarse grained or fine grained soil).
LDAT Land Damage Assessment Team	The engineering team that carried out site by site inspections of residential dwelling foundations around Canterbury to provide information for the dataset dwelling foundation damage. At the end of December 2011, approximately 75,000 inspections have been undertaken on 60,000 properties. Around 15,000 properties had inspections repeated after earthquake events followed the original inspection.

LiDAR Light Detection and Ranging	Used here to measure ground surface elevation from a plane (an aerial survey).
Liquefaction related elevation change	The LiDAR measured liquefaction related elevation change <i>damage attribute</i> which has had the tectonic component removed.
LPI Liquefaction Potential Index	Iwasaki's 1978 parameter indicating vulnerability to liquefaction effects.
LSN Liquefaction Severity Number	A new parameter to indicate the liquefaction related vulnerability of residential dwellings.
MBIE Ministry of Building Innovation and Employment	The government department that administers the Building Act. It includes what was previously the Department of Building and Housing (DBH).
Median groundwater	The median depth to the groundwater table based on the work undertaken by T&T and GNS. This represents the median groundwater level considering both summer and winter conditions.
PGA Peak Ground Acceleration	Used here as the peak horizontal ground acceleration that occurs during seismic shaking.
Potential	Whether the soil has the geotechnical characteristics such that it could theoretically liquefy if subjected to sufficient seismic loading. Potential has not changed in Canterbury as a result of the earthquake series as the soil characteristics have not substantially changed.
QPID Quotable Value Property Identification	A unique number that identifies a residential property.
R&W or RW Robertson & Wride	Used here to refer to the calculation of apparent fines content based on CPT results.
Residential Red Zone	An area defined by the Government as unsuitable for continued residential occupation at the present time. Generally this area encompasses the most severely damage land in Canterbury. Identified in this report as being highly vulnerable to liquefaction hazard.
S Calculated settlement indicator	A <i>calculated parameter</i> of settlement deformation, calculated using the Zhang et al. (2002) method (see ZRB).

SLS Serviceability limit state	The 25 year return period design earthquake loading for residential structures. Structures are expected to be designed to experience little to no damage under SLS conditions. This is modelled as a 0.13g, M7.5 earthquake load.
SPT Standard Penetration Test	In situ dynamic penetration test expressed as a number (the SPT-N value). Denser and stiffer materials have higher numbers.
Susceptibility	The seismic loading (shaking) required to trigger liquefaction. Susceptibility of soil layers to liquefaction triggering has not changed in Canterbury as a result of the earthquake events because the soil strength properties have not substantially changed.
TC2 Technical Category 2	A classification of land susceptible to liquefaction developed by the NZ Department of Building and Housing for foundation investigation purposes.
TC3 Technical Category 3	A classification of land susceptible to liquefaction developed by the NZ Department of Building and Housing for foundation investigation purposes.
Tectonic movement	Regional change in ground elevation induced by earthquake displacements in the underlying bedrock.
UoC PGA	Interpolated ground acceleration distributions from Dr Brendon Bradley at the University of Canterbury (Bradley, 2012a-c). UoC is used in this report as a shorthand for the acceleration distributions prepared by Dr Bradley.
ULS Ultimate limit state	The 500 year return period design earthquake loading for residential structures. The structure is expected not to collapse under ULS conditions. This is modelled as a 0.35g, M7.5 earthquake.
Vulnerability	The consequence of triggered liquefaction at the ground surface on residential land in Canterbury. Vulnerability has changed as a result of ground surface subsidence, as the ground surface moves towards the groundwater table and consequently the depth to potentially liquefiable materials decreases (i.e. the crust thickness reduces). The closer the potentially liquefiable deposits are to the ground surface, the more vulnerable the property is to the liquefaction hazard.
ZRB Zhang Robertson & Brachman	A method for calculating volumetric densification.

1 Introduction

1.1 Objectives

The Canterbury area has been affected by a large number of earthquakes following the main earthquake on 04 September 2010. These earthquakes have caused widespread liquefaction, lateral spreading and ground surface subsidence. The liquefaction and lateral spread caused extensive damage to residential dwellings and infrastructure in large areas of Christchurch. In other areas of Christchurch there was only minor liquefaction related damage even though liquefaction of some of the soil layers has most likely occurred.

The liquefaction related land and dwelling damage during the recent earthquake series in Canterbury has highlighted the need to better understand the vulnerability of land to liquefaction damage caused by future earthquakes. Tonkin & Taylor (T&T), on behalf of the Earthquake Commission (EQC), have carried out a review of liquefaction vulnerability parameters used to predict liquefaction damage and to assess how they compare with the observed damage. The objectives of the study are to determine a liquefaction parameter that is suitable for predicting liquefaction vulnerability in Canterbury. The findings of this study can also be applied to areas beyond Canterbury, but consideration will need to be given to the different soil conditions in other areas that may not perform in the same way.

This report is intended to be read in conjunction with the appendices, and in particular the figures presented in Appendix A. It is strongly recommended that the appendices be viewed in a separate document that can be considered at the same time as the text.

1.2 Outline

The liquefaction vulnerability assessment presented in this report is based on a detailed study comparing measured *damage attributes* (land damage, dwelling foundation damage and liquefaction related elevation change datasets), mapped and measured after each main earthquake in the Canterbury Earthquake series to the liquefaction vulnerability indicators (*calculated parameters*) of the Liquefaction Potential Index (LPI), calculated settlement indicator (S) and a new calculated parameter developed by Tonkin & Taylor Liquefaction Severity Number (LSN) for the main earthquakes. The calculated parameters are based on the groundwater levels at the time of each earthquake and the shaking intensity experienced. Figure 1 provides an overview of how the different components of this study are linked.

The geotechnical investigations that were used to analyse the calculated liquefaction vulnerability parameters included boreholes, geophysical testing and around 800 monitoring wells and 7,500 Cone Penetration Tests (CPT) available on the Canterbury Geotechnical Database (CGD) by the time the analyses in this report were undertaken. The CPT results have been combined with groundwater models, survey data and models of earthquake shaking distribution to allow the calculation of most of the liquefaction vulnerability indicators (*calculated parameters*) for earthquakes experienced in Canterbury known to have caused surface manifestation of liquefaction. These included the 04 September 2010, 22 February, 16 April, 13 June and 23 December 2011 earthquakes.

A series of data analyses have been undertaken to determine which of the three *calculated parameters* best fits all the *damage attribute* sets for each of the three main earthquakes for which damage data has been collected (04 September 2010, 22 February and 13 June 2011). A visual assessment has been undertaken of the *calculated parameters* for the other earthquakes for which there were no detailed liquefaction observations. A review of the data shows that LSN provides a better correlation with the observed damage compared to LPI and the calculated settlement indicator. On the basis of the analysis of datasets, the LSN is assessed as providing a

significantly better differentiation of liquefaction damage between the residential Red Zone, TC3 and TC2 areas compared to the calculated settlement.

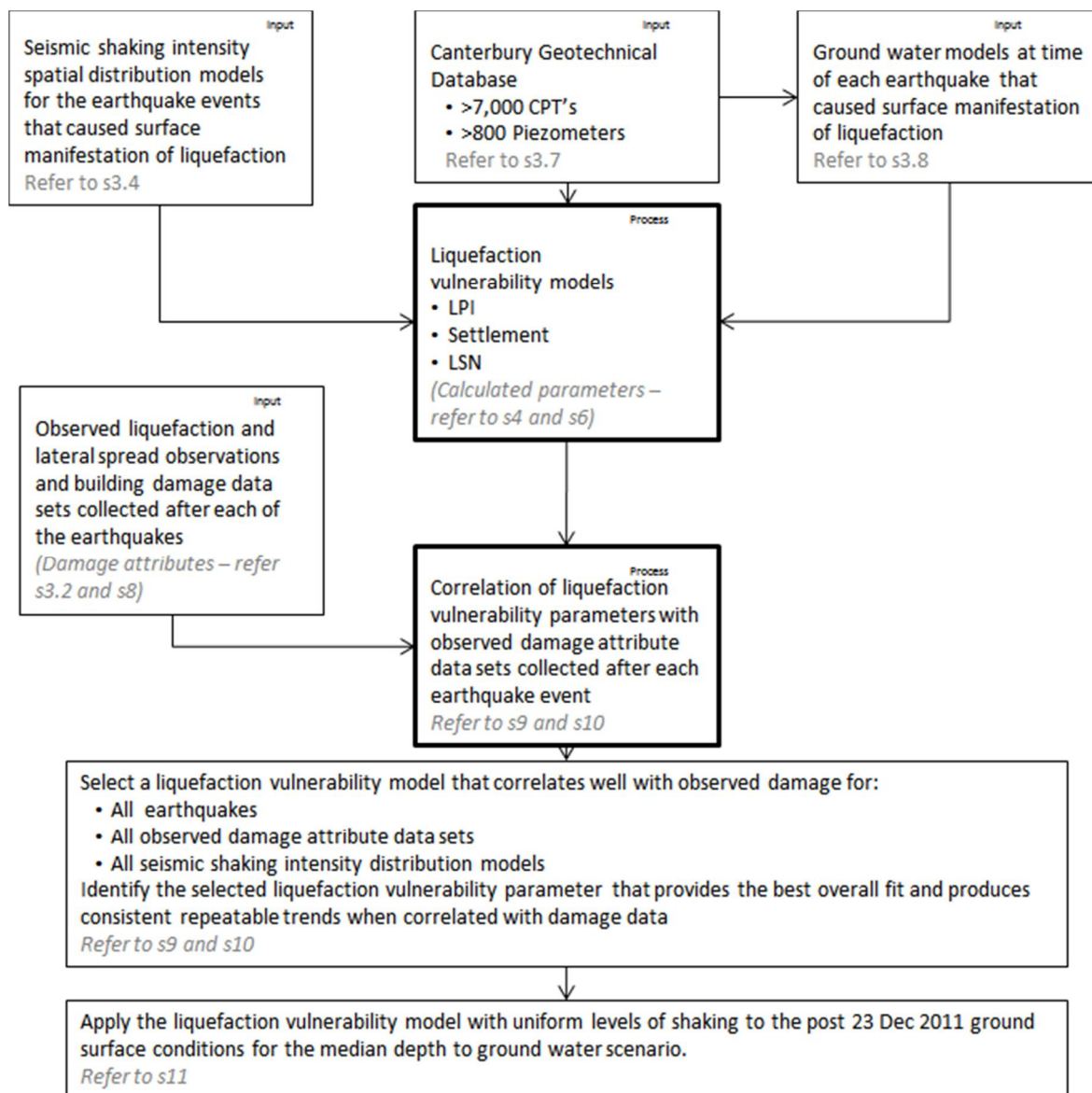


Figure 1 Liquefaction vulnerability assessment process

Section 2 provides some background to the Canterbury earthquakes, their effects and the MBIE technical categories (TC) for the different land areas. Section 3 presents damage mapping and site investigation field data, including a discussion of models for the spatial variation of earthquake ground accelerations from each of the earthquakes and groundwater depths. These models form the input data for the liquefaction triggering methods which are presented and discussed in Section 4. Section 5 summarises a review of existing literature relating to the vulnerability of sites to liquefaction and includes an initial comparison of existing tools with observations in Canterbury. Section 6 presents a discussion of the parameters calculated from the triggering methods, followed in Section 7 by an assessment of the response of typical CPT from the residential Red Zone, as well as from TC3 and TC2 areas. Section 8 comprises a discussion on the dataset construction and interpolation methods used in the analyses. The results of the analysis for the main earthquakes are presented and discussed in Section 9, with the results for smaller aftershocks presented in Section 10.

The calculated performance of the land in future earthquakes is presented in Section 11, along with the sensitivity analyses to changes in groundwater conditions. Section 12 presents discussion of LSN and lateral spread. Photographs of typical examples of sites with various LSN are discussed in Section 13. Section 14 presents an interpretation of calculated LSN values with a summary and conclusions in Section 15.

The report concludes that, on the basis of the analysis of datasets related to the Canterbury earthquake series, LSN provides a suitable tool to assess the vulnerability of residential properties to future land damage resulting from liquefaction.

1.3 Applicability

This report presents the results of a study of liquefaction vulnerability in the Canterbury region. The following organisations and people may find this liquefaction vulnerability study particularly useful:

- (a) Ministries, and in particular the Ministry of Business, Innovation and Employment
- (b) Local and regional councils
- (c) Government departments, and in particular the Earthquake Commission
- (d) Insurers
- (e) Consulting engineers
- (f) Researchers and scientists

While the vulnerability study presented herein can be used for a variety of purposes, it is important that anyone using this data understands the limitations and assumptions that relate to this report. Readers should carefully review and understand this document before using the methods and information presented here.

The liquefaction land damage vulnerability study presented here may be used for a variety of purposes and it is important to understand the limitations and assumptions that relate to this study. It is the sole responsibility of those using any aspect of this report to satisfy themselves that the methods and information presented in this study are applicable to their site or project. The calculated datasets that are considered in this study are based on assumptions and interpolation between investigation points and it must be appreciated that actual conditions could vary from the inferred values.

This study is based on readily available data from the Canterbury region. The results of the study may be applicable elsewhere, but this should be carefully considered by those considering the study. Analyses of liquefaction are based on published methods. It is important to note that these methods are probabilistic rather than deterministic (i.e. they generate an indication of the degree of risk rather than a definitive result). It is important that engineering judgment be used in interpreting the results of these analyses.

This document is released for general information purposes only and should only be used for design purposes by appropriately qualified and experienced Scientists, Geologists and/or Professional Engineers.

All the data and information which is contained in this document may only be used for the purposes of recovery and repair of land and building damage associated with the Canterbury Earthquakes. This report comprises a main body and separate appendices which must be read in their entirety and are to be used on conjunction with each other.

This report has been prepared for the benefit of the Earthquake Commission with respect to the particular brief given to us and it may not be relied upon in other contexts or for any other purpose without our prior review and agreement.

2 Background

2.1 Canterbury earthquakes and liquefaction

The Canterbury region has been affected by a large number of earthquakes following the main earthquake on 04 September 2010 causing widespread liquefaction, lateral spreading and ground surface subsidence. The location of each of the main earthquakes and aftershocks is shown on Figure A1. Detailed mapping of liquefaction and lateral spreading observations were carried out for three of the most severe earthquakes (refer Figures A3, A4 and A7), which are denoted by an asterisk in Table 2.1. LiDAR surveys were also undertaken after each main earthquake (Figures A15-A19). The difference between the surveys (refer Figures A20-A31) represents the change in ground surface elevation recorded between earthquakes. The figures show the tectonic correction that has been applied to the data.

Table 2.1 Summary of earthquakes where surface manifestation of liquefaction was observed

Earthquake	Date	Modelled Magnitude	Depth and Location
Darfield Earthquake (*) (Greendale)	04 September 2010	7.1	10 km deep, 35 km W of Christchurch
Christchurch 1 Earthquake (*) (Lyttelton)	22 February 2011	6.2	5 km deep, 10 km SE of Christchurch
Aftershock	16 April 2011	5.3	11 km deep, 20 km SE of Christchurch
Christchurch 2 Earthquake (*) (Sumner, 2 events)	13 June 2011	6.2 ¹	9 km deep, 10 km SE of Christchurch; 6 km deep, 10 km SE of Christchurch
Christchurch 3 Earthquake (New Brighton, 2 events)	23 December 2011	6.1 ²	8 km deep, 20 km E of Christchurch; 6 km deep, 10 km E of Christchurch

* indicates significant earthquakes for which detailed land damage mapping was undertaken.

Note 1 The combination of earthquakes was modelled as magnitude 6.2. Refer to Section 3.4

Note 2 The combination of earthquakes was modelled as magnitude 6.1. Refer to Section 3.4

The 23 December 2011 earthquakes also caused substantial land damage around Christchurch, including the manifestation of liquefaction, lateral spreading and land subsidence. Detailed land damage mapping was not undertaken for this earthquake because rapid mapping undertaken in the days immediately after the earthquake (Figure A8) indicated that patterns of land damage were generally similar to that mapped in detail for the previous earthquakes.

There are two other earthquakes that resulted in surface manifestation of liquefaction. However, these surface manifestations were minor in comparison with the larger earthquakes and much smaller in extent. These earthquakes did not result in measurable ground surface elevation changes. The surface manifestation of liquefaction during an earthquake on 19 October 2010 was generally confined to localised areas in Hoon Hay and Halswell. This earthquake was not modelled and so is not presented in Table 2.1.

The surface manifestation of liquefaction mapped during an earthquake on 16 April 2011 as well as the first earthquake on 13 June 2011 (Event A, magnitude 5.6) was based on visual observations from a rapid drive-by inspection. Observations based on the areas that were inspected were generally confined to the current residential Red Zone areas adjacent to the Avon

River. Maps showing the location of surface expression of liquefaction for the 16 April and 13 June 2011 (Event A) earthquakes are shown on Figures A5 and A6.

The ground surface subsidence that has occurred in affected parts of Canterbury is attributed to a combination of the following:

- (a) Regional tectonic subsidence,
- (b) Densification of underlying materials,
- (c) Vertical subsidence resulting from lateral spreading or slumping (topographic effects),
- (d) Ejection of subsurface materials associated with liquefaction to the ground surface. This usually manifests at the ground surface as sand boils.

2.2 Regulatory framework

MBIE have categorised land in Canterbury into three categories depending on the level of specific engineering assessment required for repair or rebuilding (MBIE, 2012). The categories are largely based on visual observations of land performance from the 04 September 2010 and 22 February 2011 land damage mapping observations. Since then, additional damage datasets have become available which provide additional information on observed land performance. These datasets included changes in ground surface elevation due to liquefaction, foundation damage mapping and additional land damage observation maps from other earthquakes. In the 2012 MBIE guidance document (MBIE, 2012) the three technical categories are:

- TC1: Future land damage from liquefaction is unlikely, and ground settlements from liquefaction effects are expected to be within normally accepted tolerances. Once the technical category is confirmed, shallow geotechnical investigations may be required (depending on the degree of damage, and in particular for a rebuild). If the 'good ground' test is met, NZS 3604 foundations (as modified by B1/AS1) can be used.
- TC2: Liquefaction damage is possible in future large earthquakes. Shallow geotechnical investigations may be required (depending on the degree of damage, and in particular for a rebuild) and, subject to establishing minimum bearing capacities, suspended timber floor or enhanced slab foundation options can be used.
- TC3: Liquefaction damage is possible in future large earthquakes. Deep geotechnical investigation (or assessment of existing information) may be required (depending on the degree of damage, and in particular for a rebuild) and depending on the geotechnical assessment, might require specific engineering input for foundations.

The guidance report states that the technical categories are intended to guide foundation solution developments at each site. The nominal criteria used to define the technical categories is presented in Table 2.2 below. They are typically based on criteria under serviceability limit state (SLS) and ultimate limit state (ULS) earthquake loadings. Areas may also be classified to a technical category based on their lateral spread risk, the assessment of which falls outside the scope of this report.

Table 2.2 MBIE technical category classification

Foundation technical category	Future land performance expectation from liquefaction	Nominal SLS land settlement	Nominal ULS land settlement
TC1	Liquefaction damage is unlikely in a future large earthquake	0 – 15 mm	0 – 25 mm
TC2	Liquefaction damage is possible in a future large earthquake	0 – 50 mm	0 – 100 mm
TC3	Liquefaction damage is possible in a future large earthquake	>50 mm	>100 mm

The MBIE (2012) guidance report states that the settlement should be calculated based on Idriss and Boulanger triggering (2008), with deformation settlements based on Zhang, Robertson and Brachman's work (2002). MBIE does not suggest that these are the best methods, but rather suggest a single method be used to provide consistency across assessments.

3 Field investigations and damage mapping

3.1 General

This section presents a brief summary of the liquefaction and lateral spreading observation mapping as well as the foundation damage mapping and LiDAR ground surface subsidence undertaken to produce the observed *damage attribute* datasets. The section also summarises the analyses presented in Section 9 of this report.

3.2 Mapped land and dwelling foundation damage attributes

3.2.1 Mapped land damage attributes

Following each of the main earthquakes listed in Table 2.1, a qualitative mapping exercise of liquefaction and lateral spreading observations was carried out. The assessments comprised a staged global assessment of the severity of liquefaction observation throughout the wider Christchurch region based on surface observations of liquefaction.

Property or road scale maps showing categorised quantities of ejected material and lateral spreading observed after the 04 September 2010, 22 February 2011 and 13 June 2011 (combined event) earthquakes are presented on Figures A3 and A4 and A7.B. The definitions for the various observation categories are presented on Figures A2.A and A2.B.

Observations of the quantities of material ejected due to liquefaction and observations of lateral spreading were collated from rapid (walkover) inspections of individual properties following each significant earthquake. The observations were categorised according to the quantity of ejected material observed on the ground surface and according to the presence or absence of evidence of lateral spreading. Each of these categories was further subdivided according to severity.

The observations were only made in residential areas of greater Christchurch. The mapping only identified ejected material and lateral spreading that was visible at the ground surface at the time of inspection. Liquefaction may have occurred at depth without obvious evidence at the surface and evidence of liquefaction may have been removed before the inspection. Material that was

removed prior to the rapid inspections can still be identified on the aerial photographs that were taken within a day or two of the earthquakes.

The rapid mapping did not cover all properties in Christchurch after each earthquake, so the extent of the mapped liquefaction and lateral spreading observations is not complete. Also, some of the evidence observed following the 22 February 2011 and 13 June 2011 earthquakes could have been caused by damage from preceding earthquakes.

The majority of the mapping was generally undertaken within a fortnight of each earthquake and was carried out by a small team of experienced Geotechnical Engineers and Engineering Geologists. The field teams regularly cross checked their mapping work to ensure consistency in the data that was gathered.

After the 04 September 2010 earthquake, the observation mapping was triaged into the worst affected areas. The mapping proceeded from the worst affected areas outwards and stopped once areas with no apparent damage were identified. These 'no damage' areas are mapped as blue on Figure A3. The non-coloured area of this map shows areas where mapping was not undertaken but generally comprised areas where no surface effects from liquefaction were observed or reported.

The same exercise was repeated after 22 February 2011 (see Figure A4). It is noted that while there was reported minor quantities of ejected material observed in the northern suburbs (e.g. Spencerville, Brooklands, Kaiapoi, Pines and Kairaki), by the time the mapping team got to these areas the ejected sand had already been removed, and hence mapping was not undertaken after 22 February 2011 in these areas.

The same exercise was not repeated after the 13 June 2011 earthquake. Instead, a more rapid road survey based on the same criteria was undertaken (Figure A7.A). The observations were then interpolated in order to assign a damage category to each property (Figure A7.B).

3.2.2 Mapped dwelling foundation damage attributes

The liquefaction and lateral spreading observations mapping was followed by a detailed inspection of liquefaction induced land damage for EQC land damage claim assessment purposes within the insured envelope of residential properties around Canterbury. In addition, these detailed inspections also included visual assessments of dwelling foundation damage. The inspections were carried out by the Land Damage Assessment Team (LDAT) which included a pool of around 400 Geotechnical Engineers and Engineering Geologists overseen by T&T. The LDAT data was recorded on standardised forms. Figure A9 shows the part of the form used to record the visual assessment of dwelling foundation damage. The detailed individual property assessment exercise commenced in September 2010 and was generally completed by December 2011. The results of approximately 75,000 inspections are shown on Figures A10-A14.

The reliability of the various attributes including the observed dwelling foundation damage is discussed in Section 8.3. The quality of the foundation *damage attribute* reduces through the earthquake series as the damage is not typically repaired and so some or all of the damage may be caused by previous earthquakes. As a result, while the damage indications are important, they can be less reliable than the land *damage attribute* that is removed and effectively 'resets' after each earthquake. Maps showing the foundation *damage attribute* are presented on Figures A11 – A14.

3.2.3 Residential Red Zone

Areas of land have been identified by the government as being so badly damaged by the earthquakes that it is unlikely they can be rebuilt on for a prolonged period. These areas have been zoned as 'Red Zone' land by the Government. The locations of the Red Zones, as of March 2012, are shown on a map produced by the Canterbury Earthquake Recovery Authority (CERA, 2012) and can also be identified on the CPT location map (Figure A36).

3.3 Correlation between land and dwelling foundation damage attributes

The indicators considered in this report relate primarily to the vulnerability of residential land to adverse liquefaction related damage. The liquefaction and lateral spreading observations made after each earthquake are considered to be the most reliable *damage attribute* for the purposes of correlation with the *calculated parameters* considered. The relative reliability of *damage attributes* is discussed further in Section 8.3. It is noted that there is a strong correlation between liquefaction and lateral spreading observations and dwelling foundation damage. This observation has been cross-checked by plotting mapped liquefaction and lateral spread observations against dwelling foundation damage. The results of this are shown in Figure G1.

Bubble plots show three different variables on a single graph. Dwelling foundation damage and land damage are plotted against each other for the three earthquakes considered. The land damage is on the x-axis, while dwelling foundation damage is on the y-axis. The size of the bubble represents the percentage of properties with some minor, moderate and severe foundation damage for a particular land observation category. The sum of vertical series adds to 100%. The colours do not directly represent any particular variable but generally indicate the degree of damage, from low at the lower left hand side (blue, white) to severe at the upper right hand side (red).

The plots show that there is an overall positive correlation between the land damage and dwelling foundation damage observations. The number of locations where there is severe land damage and none to minor dwelling foundation damage, or vice versa, is low.

3.4 Seismic loading

The seismic loading imposed by an earthquake to trigger liquefaction is represented by the Cyclic Stress Ratio (CSR). Published literature shows CSR to be a function of the peak ground acceleration (PGA). PGA were measured in ground shaking records around Christchurch by seismographs operated by GeoNet (a subsidiary of GNS Science). The spatial variation of the PGA between monitoring stations for the earthquakes listed in Table 2.1 has been considered by two research groups. Mr. Milashuk and Prof O'Rourke at Cornell University (Cornell) have modelled the spatial variation by contouring the results of the geometric mean ground accelerations using a Kriging interpolation method. The results of their work have been presented in O'Rourke and Milashuk (2012) and Milashuk (2012).

Dr Bradley at Canterbury University (UoC) has also carried out an assessment of the PGA distribution by assessing conditional distributions of PGA based on an empirical ground motion prediction equation. The method is set out in the Bradley (2012b-c). The spatial distribution of PGA for the earthquakes listed in Table 2.1 using the two approaches are presented on Figures in Appendix F.

The 13 June and 23 December 2011 aftershocks each comprised two separate earthquakes within 80 minutes of each other. In both cases the second of the two earthquakes was the more damaging, with extensive liquefaction and dwelling foundation damage observed. The first

earthquake is inferred to have caused elevated pore water pressures in potentially liquefiable materials in situ. Elevated pore water pressures make the material more susceptible to liquefaction in subsequent earthquakes.

For the purposes of the liquefaction assessment, the second earthquake was modelled with an increased magnitude as a means to include the effects of the initial, smaller earthquake. Based on measured dissipation of pore water pressures and the timing between the two earthquakes, a 25% contribution from the first earthquake has been adopted for modelling purposes. The basis for this assumption is discussed further in Appendix B and summarised in Table 3.1 below. The individual earthquake magnitudes used for modelling were supplied by GNS (Berryman, 2012).

Table 3.1 Design seismic loading for 13 June and 23 December 2011 earthquakes

Earthquake	Magnitudes and time	Design earthquake magnitude
13 June 2011	M5.6 and M6.0 separated by 80 minutes	M6.2
23 December 2011	M5.8 and M5.9 separated by 80 minutes	M6.1

3.5 Survey and regional deformation

The elevation of the ground surface around Canterbury has been recorded using aerial LiDAR survey. A baseline survey of Christchurch in 2003 was commissioned by Christchurch City Council, with additional surveys flown after each of the main aftershocks. Flown LiDAR is a GPS based survey that produces data in GPS-space (i.e. with absolute X, Y, Z points relative to the satellite network). The LiDAR was typically undertaken a month after each main earthquake (with the exception of the post September 2010 LiDAR which was flown the day after the earthquake). This allowed time for ejected sand and silt to be removed from most sites to allow the measurement of actual changes to the ground surface level. The extent of LiDAR coverage varied after each earthquake and covered areas believed to have been affected by ground surface subsidence.

LiDAR was acquired by AAM Brisbane (AAM) and New Zealand Aerial Mapping (NZAM) following each of the significant earthquakes. The suppliers classified the acquired points allowing the creation of a bare earth or terrain model, by removing points for structures and vegetation that were judged to be higher than 0.5 m above the surrounding ground. A Digital Elevation Model (DEM) was developed from each supplied LiDAR set by averaging the ground-return elevations within a 10 m radius of each grid point. All of these DEM's used a common 5 m grid and used either moving averages or windowed averages. Each DEM was colour banded and rendered in an image pyramid to create a viewable version of the underlying elevation model. Significant waterways and coastal marine areas were clipped from the colour images.

The LiDAR sources and commissioning agencies are set out below in Table 3.2.

Table 3.2 LiDAR Source and Commissioning Agencies

DEM	Source LiDAR	Commissioning Agencies
Pre-Earthquake	AAM, 6-9 Jul 2003	Christchurch City Council
	AAM, 21-24 Jul 2005	Environment Canterbury & Waimakariri District Council
	AAM, 6-11 Feb 2008	Environment Canterbury & Selwyn District Council
Post-Sept 2010	NZAM, 5 Sep 2010	Ministry of Civil Defence and Emergency Management
Post-Feb 2011	NZAM, 8-10 Mar 2011	Ministry of Civil Defence and Emergency Management
	AAM, 20-30 May 2011	Christchurch City Council
Post-June 2011	NZAM, 18 & 20 Jul, 11 Aug, 25-27 Aug, and 2-3 Sep 2011	Earthquake Commission
Post-Dec 2011	NZAM 17-18 Feb, 2012	Earthquake Commission

The bare earth model has enabled comparisons of ground surface elevation to be made for some areas after each of the main earthquakes. Appendix A presents copies of the ground surface elevations measured by LiDAR prior to September 2010 and after each of the four main earthquakes (Figures A15-A19). Elevation changes were calculated both for individual earthquakes (and their associated aftershocks) and for sets of consecutive earthquakes as differences between LiDAR sets.

The ground around Canterbury has experienced regional scale tectonic movements caused by the earthquakes. These movements comprise both translation and elevation change which have deformed the ground surface. After each major aftershock, Land Information New Zealand (LINZ) re-surveyed a network of survey benchmarks around Canterbury. This survey re-established the location of the benchmarks relative to the rest of the physical survey network around New Zealand and allowed GNS to assess regional vertical tectonic deformation movements (Beaven 2010, 2011, 2012). This has also allowed the comparison of the elevation of GPS based LiDAR points and ground based survey points to be made. The correction has also allowed the local effects of liquefaction induced elevation change (the ejection of sand, lateral spreading, topographic effects and the settlement of liquefied soils) to be isolated from tectonic ground movements. Appendix A presents copies of:

- (a) the cumulative change in ground surface elevation after each earthquake relative to pre-September 2010 (Figures A20-A23)
- (b) the cumulative tectonic change after each earthquake relative to pre-September 2010 (Figures A24-A27)
- (c) the cumulative change in ground surface after each earthquake due to liquefaction related effects by subtracting the vertical tectonic movement from the corresponding change in ground surface elevation (Figures A28-A31)

All of the ground surface elevation change maps are derived from differences between DEMs. The post-Feb 2011 DEM was created from two partially overlapping LiDAR sets, with points taken from the more accurate set wherever the two sets overlapped. Some of the DEMs have visually distinguishable lines or ripples within the colour bands that are almost certainly artefacts from the data acquisition and subsequent processing rather than representing physical vertical movements. Notable examples are several approximately NNE-SSW swathes visible in Figure A28, and an almost E-W line at 43.48°S shown on Figure A29.

Metadata supplied with the source LiDAR indicates the survey equipment had a vertical accuracy of ± 0.15 m for the 2003 survey and ± 0.07 m for the subsequent surveys. These errors exclude GPS error and Geoid modelling error and have a horizontal error of 0.40 to 0.55 m. The pre-earthquake LiDAR has lower accuracy and sparser LiDAR point sets than the post-earthquake sets. All of the LiDAR elevation measurements within a 1 m radius of each benchmark were extracted from the data, and the elevation compared to the re-surveyed benchmark elevation surveyed by LINZ. The elevation difference between each measurement point and the benchmark were plotted over an aerial photograph, and points that were clearly not ground surface measurements (e.g. fence tops, vegetation, cars etc.) were removed from the dataset. All of the differentials were then analysed and plotted on the LiDAR elevation maps (Figures A15-A19) to show the spatial distribution of the measured differences. The average and standard deviation between the measured LiDAR observations and the corresponding survey benchmark elevations are presented in Table 3.3.

The final elevation differences still include unquantified errors associated with the elevation difference between the benchmark and its surrounding ground. This includes differences associated with local features such as kerbs and other depressed or raised surfaces.

Table 3.3 LiDAR set survey elevation verification statistics

LiDAR set	Average error (mm)	Standard deviation of the error (mm)
2003	-11	158
September 2010	-8	56
February 2011	8	59
May 2011	46	61
June 2011	-19	70

Horizontal ground movements

Horizontal movements were calculated for both individual earthquakes (and their associated aftershocks) and sets of consecutive earthquakes as differences between pairs of LiDAR point clouds relative to pre-September 2010. The horizontal movements for each earthquake combination were calculated using a sub-pixel correlation method developed by Imagin'Labs Corporation and California Institute of Technology. The movements were calculated on 4 m grids (8 m for the pre-earthquake LiDAR sets) from both ground and non-ground LiDAR points and averaged to provide Cartesian movements in a 56 m grid. The averaging distance was tailored to the noise in between each LiDAR pair.

The horizontal movements were rendered as arrows on a 56 m grid to indicate both direction and magnitude of the movement at each grid point. The arrows were scaled 56:1 so an arrow between two adjacent grid points (e.g. east-west or north-south) represents 1.0 m movement in the indicated direction. Arrows were not plotted in significant waterways, coastal marine areas and most other non-residential land where the movements were poorly correlated and produced less accurate horizontal movement estimates. The correlation process and horizontal movements are also significantly affected by elevation errors. Some of the horizontal movement are also

influenced by localised changes such as new or demolished buildings, vegetation and earthworks for subdivisions.

The horizontal movements were validated with data supplied by the Christchurch City Council, Land Information New Zealand and Environment Canterbury from surveys of their benchmark networks. This validation comprised comparing the vector results with calculated movement vectors from re-surveyed benchmarks. The two deformation results generally agreed with respect to direction and magnitude.

'Local' horizontal deformations were calculated as the differences between the 'observed' movements obtained from the LiDAR vectors and the associated horizontal movements from the tectonic models (i.e. horizontal movement at the ground surface with the horizontal tectonic movements subtracted). The horizontal movements as well as the tectonic movements are represented in Figures A32.

3.6 Other mapping

In addition to the liquefaction and lateral spread observation mapping, crack locations have been mapped in order to infer the general direction, magnitude and extent of the lateral spreading. Field observations of crack locations were recorded using coloured pens on paper copies of aerial photographs. The marked-up photographs were later scanned manually digitised.

The mapping objectives changed in response to the varying situation following the two main earthquakes. Observations after the 04 September 2010 earthquake were principally for EQC claim settlement purposes. The crack widths were recorded based on individual property observations, but cracks were not tracked across property boundaries and only a portion of damaged properties were mapped before the 22 February 2011 earthquake.

Cracks were mapped at a scale of 1:5,000 to 1:10,000 for approximately two weeks following the 22 February 2011 earthquake in order to rapidly identify the extent of lateral spreading following the earthquake. The individual crack widths were not recorded.

From early March 2011, cracks were generally mapped at a scale of 1:2,000 and classified according to their maximum width (with many tapering to nothing at both ends). Cracks were tracked through properties in order to identify spreading regions rather than spreading within individual properties.

The crack mapping is incomplete and only observations made by the mapping teams are presented. In particular, the mapping following the 04 September 2010 earthquake had not been completed before the 22 February 2011 earthquake occurred and subsequent mapping remains incomplete within the residential 'Red Zone' areas. Also, cracks in roads were often not able to be mapped because many were filled and the roads resealed before a mapping team arrived.

The crack mapping is shown in Figures A34 and A35. The resultant horizontal movement vectors discussed in Section 3.5 are overlaid on the crack map (Figure A33).

The data described in this section is discussed for information only, and has not directly been used in the regional assessment of liquefaction.

3.7 Geotechnical investigations

Following the 04 September 2010 earthquake, EQC commissioned geotechnical ground investigations in areas of Canterbury affected by consequential liquefaction. These investigations were largely completed when the 22 February 2011 earthquake occurred and were primarily scoped to design government funded ground improvement works along the waterways to improve the land and mitigate the future potential for lateral spreading. The 22 February and 13 June 2011 earthquakes resulted in a larger area of land that was affected by consequential liquefaction and a geotechnical investigation with a wider scope was commissioned by EQC. In addition, Christchurch City Council commissioned a comprehensive geotechnical investigation in the central business district of Christchurch City. The site investigations typically comprised:

- (a) Cone penetration testing with dynamic pore pressure measurement (CPT)
- (b) Borehole drilling with selected laboratory testing
- (c) Geophysical testing primarily comprising multichannel analysis of surface waves (MASW)
- (d) Review of the Environment Canterbury borehole database (ECan)
- (e) Construction of piezometers for groundwater monitoring

A further geotechnical investigation at closely spaced intervals is being carried out by EQC, private insurers and property owners in areas of land identified by the MBIE as requiring further geotechnical investigation for foundation design. This investigation is likely to comprise between 10,000 to 15,000 CPT and 1,000 to 2,000 boreholes.

The CPT soundings are the primary tool used in this report to calculate liquefaction related parameters (discussed in Section 6). A plan showing the locations of CPT soundings carried out to date and considered in this report are shown on Figure A36. Only CPT with depths in excess of 5 m were used in this analysis. The results of the groundwater monitoring and subsequent modelling carried out are discussed in Section 3.8. Locations of selected CPT and boreholes adjacent to each other (CPT/borehole pairs) are shown on Figure A37.

3.8 Groundwater design models

A regional groundwater model has been developed to provide a basis for geotechnical liquefaction modelling around Christchurch at the time of the earthquakes. The groundwater model used for liquefaction analysis represents elevation contours of the surface of the water table for the greater Christchurch area.

The models used in this report are based on groundwater level data from over 800 monitoring wells, the locations of which are shown in Figure C1. Four earthquake-specific groundwater surfaces have been developed based on the median water table surface which was created for greater Christchurch, as summarised in van Ballegooy et al. (2013). The median water table surface is presented in Figure C1 and the depth to groundwater is presented in Figure C2. The median water table surface was used to develop earthquake specific water table surfaces for the four earthquakes listed below, for which further discussion is provided below and in Appendix C.

- a) 04 September 2010
- b) 22 February 2011
- c) 13 June 2011
- d) 23 December 2011

Monitoring well data from the following sources contributed to the development of the median water table surface:

- (a) Christchurch City Council (CCC) – 22 wells, long term (>10 year) monitoring duration, typically measured at weekly or fortnightly intervals;
- (b) Environment Canterbury (ECan) – 22 wells, long term (>10 year) monitoring duration, typically measured at weekly or fortnightly intervals;
- (c) Earthquake Commission (EQC) – 762 wells, all installed after 22 February 2011, typically measured at monthly intervals.

The total 806 monitoring wells selected for the development of the median water table surface, are assumed to provide data on the unconfined water table (as opposed to confined aquifers). To qualify as being representative of the surface water table, all monitoring wells were required to be either:

- (a) a shallow depth (<10 m) in the Eastern/Coastal or Transitional zones, with groundwater levels that are not locally anomalous; or
- (b) an intermediate depth (from <10 to 35 m) in the Inland Zone, west of Christchurch City where the groundwater is unconfined and Weeber (2008) demonstrated connection between the shallow aquifers.

Any monitoring well records that appeared to be measuring confined groundwater levels, indicating either artesian or sub-artesian pressure, were not included in the dataset used to generate the median water table surface.

In addition to monitoring well data, monitored river level data for the Avon, Heathcote and Styx Rivers (provided by CCC), and river level data for the Waimakariri River (provided by ECan) contributed to the development of the median water table surface. A mean sea level along sections of coastline on the study area's eastern extent was also assumed for the generation of the median water table surface.

Appendix C describes the process whereby the median water table surface was used to create earthquake specific surfaces for four earthquakes. Earthquake-specific groundwater elevation surfaces have been developed for the four earthquakes listed below.

- (a) 04 September 2010 (Figure C4)
- (b) 22 February 2011 (Figure C6)
- (c) 13 June 2011 (Figure C8)
- (d) 23 December 2011 (Figure C10)

The subsequent use of the models for liquefaction analyses assumes a hydrostatic pressure regime beneath the water table surface for the upper materials relevant to residential liquefaction analyses.

The depth to groundwater immediately prior to each earthquake was calculated (and used for the liquefaction triggering analyses in Section 4) based on subtracting the groundwater elevation from the pre-earthquake ground surface elevation. For analysis of future earthquakes the median groundwater table has been assumed. This represents the 50th percentile groundwater condition (i.e. an intermediate level between winter and summer conditions). The elevation of the groundwater table (m RL) is presented in Figure C1 and the depth to groundwater is presented in Figure C2.

3.9 Damage attribute summary

The three *damage attributes* considered in this report comprise:

- (a) The observed liquefaction and lateral spreading attribute (also referred to as the land damage attribute)
Based on the amount of ejected material observed on the ground surface after earthquakes and any lateral spread that occurred
- (b) The dwelling foundation damage attribute
Based on site inspections by LDAT teams
- (c) The liquefaction related elevation change
Based on LiDAR settlement surveys corrected for tectonic movement

4 Liquefaction triggering

4.1 General

This section presents a brief summary of the methods used to assess liquefaction triggering in the CPT soundings around Canterbury. The *calculated parameters* of LPI, calculated settlement indicator and LSN use the Idriss and Boulanger (I&B) method, which is based on the simplified procedure first published by Seed and Idriss (1971). For this regional analysis, we have assumed that no liquefaction occurs where the calculated soil behaviour index I_c exceeds 2.6, which is discussed in more detail in Section 4.3. More information relating to the implementation of the liquefaction triggering method is presented in Appendix B.

4.2 Idriss & Boulanger

A flowchart showing the Idriss and Boulanger (2008) approach is presented in Figure B1 and is referred to in this report as the Idriss and Boulanger method, or I&B. The I&B method recommends that specific layers at a given site be characterised and a layer specific fines content assessment be developed, ideally based on laboratory testing. Given the nature of this regional analysis involving the processing of large numbers of CPT, each with multiple liquefiable layers, the assessment of fines has had to be automated. This automation process is not recommended for individual site assessments for foundation design purposes and is only applicable to this regional study.

The I&B publication notes that CPT based predictions of fines content can over-predict fines content in some situations. To assess this, we have compared 12 selected boreholes from the CGD with 12 CPT that were located within 5 m (locations shown on Figure A37). At each site, the apparent fines content was calculated in accordance with Robertson & Wride (1998) with the results presented in Figure A38. The fines content was estimated based on I_c calculated in accordance with Robertson & Wride's work. The fines content measured in the laboratory (material passing the 63 μm sieve) is plotted as points on the graph (Figure A38). It is noted that the standard fines content measured in New Zealand uses the 63 μm . However, the liquefaction databases use the 75 μm sieve (no. 200). The difference between the two methods is expected to be minor in the context of this study.

The graphs show that there is generally a good correlation between the trend of the apparent fines content calculated from CPT and the measured fines content from the borehole sampling. In general, there is agreement between areas with high or low fines content and apparent fines

content. However, as expected, there is some difference in the results with variation between the apparent and actual fines content. Our review of the scatter indicates that there are no clear geographical correlations in the variability of the estimates (i.e. the overestimates and underestimates are not concentrated in any particular area).

Despite this scatter, we consider that the Robertson and Wride (1998) apparent fines content represents a reasonable basis to predict fines content in situ for the purposes of this study. While a CPT specific layer by layer analysis based on laboratory tests would be preferable and more accurate, this has not been feasible for the sample size analysed here. We have therefore adopted the Robertson & Wride (1998) method to calculate the fines content for use with the I&B liquefaction triggering method.

4.3 Ic-based liquefaction potential

The potential for soils to liquefy tends to be related to the amount of fine grained soils present. Very fine grained soils can experience pore pressure build-up under cyclic shear straining, with consequential softening behaviour. Strain softening behaviour is not explicitly considered in this analysis.

Robertson & Wride (1998) developed an indicator for soil behaviour called the soil behaviour classification index, or I_c . Higher I_c represent soils that behave like more fine grained materials, lower I_c materials represent soils that behave like more granular soils. Their liquefaction analysis method curtailed the analysis by assuming no liquefaction occurs where I_c exceeds 2.6, with the method stating that the soil is considered too clay-rich to liquefy. The I&B method has no defined fines cut off for liquefaction and calculates a factor of safety for all soils, even those with extremely high fines contents.

To represent the behaviour of fine grained soils under cyclic shearing for the I&B method, and for the purpose of this study, soil with a calculated $I_c > 2.6$ is assumed not to be susceptible to liquefaction. For this cutoff check we have used an I_c calculated on the basis of the normalisation and I_c calculation presented in Robertson & Wride (1998).

The actual I_c cutoff for alluvial soils in Canterbury could vary from the assumed value. Accordingly, an assessment of the sensitivity to the I_c -based cutoff has been carried out. Maps have been prepared from the CPT dataset that show the total thickness of soil material with $I_c > 2.6$, for the upper 5 m and 10 m (Figures A39 and A40). The upper 5 m is the most sensitive area to surface liquefaction effects and lateral spread. On the basis of the figures, it was not considered necessary to carry out an independent assessment of the I_c -based cut-off for the various soils within regional study presented in this report. If the database was found to be sensitive to the I_c cutoff (i.e. if there is a substantial amount of material with I_c of 2.6 or more), then a more detailed review of a suitable I_c cutoff would be assessed based on the available data. This would comprise a comparison of calculated I_c with susceptibility assessments based on Bray and Sancio (2006).

4.4 Soil density

Robertson and Cabal (2010) presented a correlation between the normalised CPT tip resistance, friction ratio and density. To consider whether implementing the correlation in the regional analysis would be useful, the sensitivity of three *calculated parameters* to variations in density was assessed.

The calculated LPI, settlement indicator and LSN parameters have been calculated for a single CPT and are presented in Figure A41 as a function of the various soil densities and at two levels of seismic loading: 0.13g and 0.35g (typical SLS and ULS earthquake loadings). They show that the *calculated parameters* do not respond significantly to a variation in density. On this basis, the

regional analysis is not assessed as being sensitive to soil density and a unit weight of 18 kN/m^3 has been assumed for all soils in this study.

4.5 Thin layer correction

The literature related to the triggering methods described in Section 4.1 all recommend the use of thin layer correction calculation. Thin layer correction attempts to represent more accurately thin layers of material where the cone results can be affected by the nature of layers above or below a specific layer. All the thin layer corrections require some degree of judgement and we are not aware of any reliable automated method for carrying out this process. Accordingly, given the large number of CPT being analysed in this regional study, no thin layer corrections have been implemented. This provides a consistent approach across all CPT's and is not thought to affect the dataset significantly.

4.6 Comparison of CPT and SPT-based liquefaction triggering

A comparison of CPT and SPT (Standard penetration test) based triggering has been carried out for the I&B method. The results of liquefaction triggering for 12 borehole and 12 CPT pairs are presented in Figure A42, with the locations presented on Figure A37. The results show that for 11 of the 12 sites, the CPT and SPT triggering assessment results are broadly similar.

One of the boreholes, BH-1883, has layers of material below 10 m depth that indicates liquefaction triggering by the SPT method, but no triggering by the CPT method. The material in this layer was logged in the borehole as a fine to medium grained sand. A review of the borehole logs and readily available data was carried out to determine whether there were any obvious indicators that could explain this difference in triggering. The assessment did not lead to any clear evidence explaining the discrepancy between the CPT and SPT liquefaction triggering analyses. It is inferred, based on knowledge of drilling procedures in Christchurch, that the most likely explanation of the lower recorded SPT values and hence threshold for liquefaction triggering was caused by heave in the base of the boreholes, which can lead to reduced SPT blow counts and indicate a weaker material than is actually present. The CPT is assessed as being less likely to record lower resistance indicators than the SPT in these materials as it is not susceptible to strength loss due to heave during the sounding.

4.7 Pre-digging of CPT locations

Health and safety requirements meant that pre-digging to confirm services were not present was undertaken at a large number of CPT locations. The digging typically extended to between 0.8 m and 1.2 m below ground surface level and the base of the pre-digging was sometimes below the groundwater table. Predigging removed material from the ground which was subsequently backfilled with an uncompacted sand.

For CPT where pre-digging has occurred, the upper part of the CPT trace will have results that cannot be reliably used when assessing the potential for liquefaction in the upper layers of material. Pseudo-low strength liquefying CPT values have been assumed over the pre-drill length for analysis purposes. However, to mitigate the effects of this assumption, an interpolation of the upper materials using data from CPT within 50 m have been used. The interpolation process is described in more detail in Section 8 and Appendix E.

5 Published liquefaction vulnerability indicators

5.1 General

This section presents a summary of an initial assessment of existing tools to assess the vulnerability of land to liquefaction induced ground damage. A review of literature is presented in Section 5.2, followed by a summary of initial data comparisons and the requirement for a review of additional *calculated parameters*.

All of the relevant published assessments of liquefaction vulnerability rely on an assessment of which layers of soil liquefy within a soil profile under cyclic shearing. The liquefaction triggering assessment methods have been discussed in Section 4.

5.2 Literature review

Vulnerability indicators - crust

Ishihara (1985) published a paper containing observations on the protective effect that an upper layer of non liquefied material had against the manifestation of liquefaction at the ground surface. The paper contained graphs that plotted thickness of the upper non liquefied layer (H1), and the thickness of underlying liquefied material (H2). The data points were divided into two main categories; sites that did not have surface expression of liquefaction at the ground surface and sites that did have surface liquefaction expression at the ground surface. The paper was based on observations for two earthquakes. Dividing lines were then drawn to separate those sites which had expression of liquefaction at the ground surface from those sites where there was no observed expression of liquefaction at the ground surface.

Youd and Garris (1995) extended this concept by considering additional data and presented data and dividing curves for ranges of peak ground acceleration. Both papers showed that, for sites with any substantial thickness of liquefied material, the upper non liquefied material typically had a critical thickness, beyond which the likelihood of ground surface manifestation of liquefaction did not increase. The paper did not directly measure damage to structures, but instead considered only whether evidence of ejected material was observed at the ground surface. The conclusion drawn from these papers is that an upper layer of non liquefying material has a beneficial effect in mitigating the occurrence of sand ejection and therefore the damaging effects of liquefaction at the ground surface.

Vulnerability indicators - parameters

The vulnerability of sites to liquefaction was also considered by Iwasaki (1978, 1982) and subsequently by Juang (2005). Iwasaki's Liquefaction Potential Index (LPI) is presented as a measure of the vulnerability of sites to liquefaction effects. The LPI presents the risk of liquefaction damage as a single value (refer to Section 6.3). The papers note that LPI values can range from 0 to 100, with the following indicators of liquefaction induced damage:

LPI range	Damage
LPI = 0	Liquefaction risk is very low
$0 < \text{LPI} \leq 5$	Liquefaction risk is low
$5 < \text{LPI} \leq 15$	Liquefaction risk is high
LPI > 15	Liquefaction risk is very high

Vulnerability indicators – foundations on a non liquefiable crust

The authors are not aware of any published information relating to the quality or performance of the upper, non liquefied material in relation to damage of structures and foundations, apart from the papers presented by Cascone and Bouckavalas (1998) and Bouckovalas and Dakoulas (2007). Bouckavalas' work presents the results of modelling that considers the ability of an upper layer of fine grained soils behaving in an undrained manner, overlying liquefied material, to support loads from shallow strip or pad foundations. A critical layer thickness is defined, where the theoretical failure surface occurs completely within the upper non liquefied material. Observations in Canterbury are that the upper materials do not typically exhibit undrained behaviour because they generally are comprised of silty sand. As a result, the findings of Bouckavalas' work are not considered to be directly relevant to this study.

5.3 Comparison of damage attributes with Ishihara criteria

The datasets from Canterbury have been applied to the published Ishihara (1985) criteria. In Christchurch the soil materials do not typically divide into two discrete units of liquefying and non-liquefying materials like H1 and H2. Therefore, the non-liquefying crust thickness was plotted against the cumulative thickness of liquefying materials in the soil profile. The results are presented in Figure A43 for magnitude weighted peak ground acceleration ranges experienced at each CPT site based on the UoC PGA model up to 0.2g, 0.3g and 0.45g.

Figure A43 show that, for the Christchurch dataset, the H1 thicknesses generally plot on the side of the dividing line that would indicate likelihood of liquefaction effects at the ground surface. The graph shows that there is no clear dividing line between those sites which were or were not affected by liquefaction. Figure A44 indicates that the Ishihara criteria is not the most suitable indicator of liquefaction damage observed in Canterbury, probably due to the presence of multiple layers of liquefying material between layers of non-liquefying material.

A visual inspection of liquefaction observation, foundation damage and LiDAR subsidence maps for the datasets shows that the majority of the areas most affected by liquefaction coincide with low lying areas where the ground surface is close to the ground water table. Conversely, sites less affected by liquefaction are in areas of higher elevation where the ground surface is higher above the groundwater table. Therefore, visually the datasets do indicate that there is some correlation between liquefaction damage and crust thickness. However, in this vulnerability study, no further formal assessment of the Ishihara criteria is pursued.

The crust thickness has been compared to the damage datasets presented in Section 8 to 10 and is discussed briefly here. The results of the crust thickness dataset comparison are presented on Figure A46 for liquefaction observations and Figure A47 for dwelling foundation damage observations. The results show a moderate correlation between increasing crust thickness and reducing damage, which is consistent with the observations of both Ishihara (1985) and Youd and Garris (1995).

6 Calculated parameters

6.1 General

This section presents the *calculated parameters* used to predict damage and compare the measured *damage attributes* and provides some background on why the *calculated parameters* were selected. The following parameters were calculated for each scenario and are briefly discussed in separate sections below:

1. Liquefaction Potential Index (LPI)
2. Calculated settlement indicator (S)
3. Liquefaction Severity Number (LSN)

The parameters were calculated using the I&B liquefaction triggering method, discussed in Section 4. Each parameter is discussed in a separate section below. All the parameters are proxy indicators for damage to land and dwellings.

6.2 Liquefaction Potential Index (LPI)

The Liquefaction Potential Index (LPI) was developed and presented by Iwasaki (1978, 1982). The LPI is defined as:

$$LPI = \int_0^{20} F_1 W(z) dz$$

Where $W(z) = 10 - 0.5z$, $F_1 = 1 - \text{FoS}$ for $\text{FoS} < 1.0$, $F_1 = 0$ for $\text{FoS} > 1.0$ and z is the depth below the ground surface in metres. The LPI presented here is based on the I&B triggering method.

6.3 Calculated settlement indicator (S)

The calculated settlement indicator is based on published methods to estimate volumetric shear strains. These strains are integrated to calculate ground settlement. The MBIE(2012) documents recommend using the I&B triggering method with the Zhang et al. (2002) volumetric densification calculation, which uses a normalised tip resistance and factor of safety to estimate settlements. The Zhang et al. (2002) method predicts strain in layers where the liquefaction factor of safety is less than 2.0. The calculated settlement indicator increases as the factor of safety drops and the material approaches a liquefied state. Therefore, some settlement is calculated when FoS is more than 1 even though liquefaction triggering has not occurred.

6.4 Liquefaction Severity Number (LSN)

The Liquefaction Severity Number LSN is a new *calculated parameter* developed by Tonkin & Taylor to reflect the more damaging effects of shallow liquefaction on residential land and foundations. The equation used to calculate LSN is presented below. LSN considers depth weighted calculated volumetric densification strain within soil layers as a proxy for the severity of liquefaction land damage likely at the ground surface. The published strain calculation techniques consider strains that occur where materials have a calculated triggering FoS that reduces below 2.0. This means that the LSN begins to increase smoothly as factors of safety drop, rather than when the FoS reaches 1.0. One other aspect of LSN to note is that strains self-limit based on the initial relative density as the factor of safety drops, so a given soil profile has a maximum LSN that it tends towards as the PGA increases.

$$LSN = 1000 \int \frac{\varepsilon_v}{z} dz$$

Where ϵ_v is the calculated volumetric densification strain in the subject layer from Zhang et al. (2002). z is the depth to the layer of interest in metres below the ground surface. The LSN presented here is based on I&B triggering with ZRB volumetric densification.

7 Sample CPT and response to PGA

The *calculated parameters* have been presented in Section 6. This section presents their response when calculated from three sample CPT. The CPT selected are located in different residential areas (TC2, TC3 and residential Red Zone) and show typical responses to seismic loading for their areas. The CPT performance and *calculated parameters* for the 04 September 2010, 22 February and 13 June 2011 earthquakes have been calculated and are summarised in Table 7.1 along with land and damage observations around each of the CPT. The selected CPT locations are shown on Figure D1.

Figures D2 to D10 show the results of the triggering assessment and the calculation of the calculated settlement indicator. LPI and LSN attributes are summarised in Table 7.1 for the selected CPT. Note that all calculated parameters are truncated at 20 m depth.

The three *calculated parameters* presented in Table 7.1 were highest in the 22 February 2011 earthquake and lowest for the 04 September 2010 earthquakes. This is similar to the PGA experienced and fits the liquefaction mapping observations. All the *calculated parameters* are highest in the residential Red Zone and lowest at the TC2 site and show a broadly consistent correlation with liquefaction land damage observations for the three sites.

However, the LSN and LPI calculated parameters have a much larger difference in value (high for residential Red Zone and low for TC2 sites) reflecting the severity of liquefaction damage observed at each site. In contrast, S does not have a significant difference in value between the residential red zone and TC2 sites, which is inconsistent with the observations of land performance.

The sensitivity of the *calculated parameters* to PGA is presented on Figure D11. Both LSN and S have a gradual increase at low PGA, where the FoS drops below 2.0. Conversely, the LPI has an abrupt start where the FoS drops below 1.0. This is due to the ZRB correlations used for S and LSN. These correlations provide smooth transitions and cause the plateauing of the parameters at high PGA. Conversely, LPI is based on a '1-FoS' calculation. This has an abrupt start and cause the LPI to continue increasing at higher PGA. The field observations indicate that damage levels tend to plateau at higher PGA, which is more consistent with S and LSN.

Table 7.1 Selected CPT

CGD Identifier		CPT_165	CPT_26	CPT_9
Location		Residential Red Zone	TC3	TC2
Land damage category	04 September 2010	Minor to moderate quantities of ejected material	No observable land damage was exhibited at the site or at surrounding sites	No observations made. Aerial photographs indicate no observable land damage at surrounding sites.
	22 February 2011	Minor to moderate quantities of ejected material	Minor to moderate quantities of ejected material	Moderate quantities of ejected material
	13 June 2011	Large quantities of ejected material	Minor cracking. No observed ejected material	Minor cracking. No observed ejected material
Dwelling foundation damage category	All events	Typically major damage	Typically minor to moderate damage	Typically minor to moderate damage
PGA (g)	04 September 2010	0.18	0.18	0.19
	22 February 2011	0.51	0.45	0.52
	13 June 2011	0.27	0.28	0.31
S (mm)	04 September 2010	174	82	69
	22 February 2011	307	267	240
	13 June 2011	193	138	105
LPI	04 September 2010	10	1	1
	22 February 2011	39	24	18
	13 June 2011	17	5	2
LSN	04 September 2010	46	11	6
	22 February 2011	62	35	28
	13 June 2011	55	22	11

Based on the data here at the selected sites, LSN is a parameter that has better behaviour compared to S or LPI. The response of LPI, S and LSN for the regional analysis is discussed in Sections 8 to 10.

8 Datasets and interpolation

8.1 General

This section presents the methods for construction of the datasets comprising *damage attributes* and *calculated parameters* for correlation purposes. The dataset development and interpolation is discussed, followed by commentary on the quality and limitations of the various *damage attributes* observed and mapped in Canterbury. The *calculated parameters* considered here are the calculated settlement indicator LPI, S and LSN. The *damage attributes* comprise liquefaction and lateral spreading observations, foundation damage and liquefaction induced elevation change.

8.2 Dataset development

The *calculated parameter* datasets presented in this report are based on the liquefaction vulnerability indicators presented in Section 6, calculated at each CPT location based on the various earthquakes that have occurred.

At the time of undertaking the analyses presented in the report, the Canterbury Geotechnical Database contained approximately 7,500 CPT investigations at discrete locations around Canterbury. Approximately 2,000 CPT were less than 5 m deep and many of these CPT were terminated before encountering refusal. The CPT all vary in length, typically ranging between 1 to 25 m. For the shorter CPT, if they are used to calculate LPI, S or LSN values, then the liquefaction vulnerability contribution from the soil profile beneath the depth at which the CPT test was terminated would not be included in the calculation. This means that the actual value would be underestimated. Therefore shorter CPT have been excluded from *calculated parameter* dataset. The process for excluding short CPT are described in Appendix D.

Altogether, only 5,500 of the 7,500 CPT in the Canterbury Geotechnical Database (available at the time when the analyses for this report were undertaken) were suitable for the calculation of LPI, S and LSN. However, the 2,000 CPT that were not suitable to calculate parameters were used to add missing layers of data for other CPT when calculating parameters using a slice interpolation technique discussed in Appendix E. The interpolation is based on the natural neighbour method, which calculates Thiessen polygons and then weights them with proximity to CPT locations. The reason for selecting this method is that it provides a smooth (natural) representation without making any assumptions about the data. The adopted method is consistent with the end use of interpolating nearby locations. Additional detail on the interpolation and slice interpolation methods are presented in Appendix E.

The LSN vulnerability indicator gives a larger weighting factor to liquefying soil layers closer to the ground surface compared to liquefying layers at depth. At a depth of 10 m onwards the calculated contribution from liquefying soil layers to the LSN vulnerability parameter for most of the CPT is less than 10% of the calculated LSN value. Therefore, for comparison purposes, the calculation of LSN from CPT is based on the upper 10 m of the CPT profile, so that the calculation method of LSN at each CPT location is the same and calculated LSN values at the discrete CPT locations can be reasonably compared. This constraint was not able to be implemented to the calculation for the LPI and S parameters when the analyses presented in this report were undertaken.

Approximately 2,000 CPT in the Canterbury Geotechnical Database were predrilled typically up to a depth of 1.5 m below the ground surface. For the cases where the predrill depths are less than the depth to the groundwater table, the calculated LSN value will not be affected. However, for the cases where the predrill depth extends below the depth of the groundwater table, the calculated LSN values are affected and assumptions need to be made about the soil properties

over the predrill depth (refer to Section 4.7). In order to maximise the use of neighbouring CPT, a “LSN Slice” interpolation process has also been implemented. Appendix E provides details of how the “LSN Slice” procedure is undertaken. In summary, CPT within 50 m of each other and within a similar geological area can contribute towards the LSN layers of a CPT which do not have a LSN value due to missing CPT data either because the CPT were terminated before 10 m depth or because the CPT were pre-drilled. As a result of the slice interpolation process, LSN values are expected to be more reliable as they use contributing LSN values from neighbouring CPT instead of making assumptions that either; the layers liquefy (in the case of pre-drill) or do not liquefy (in the case where CPT terminated before 10 m depth).

The coverage of the three *damage attributes* varies between earthquakes. The mapped liquefaction and lateral spreading observation categories and liquefaction related elevation change attributes have extensive coverage around Canterbury, while the *damage attribute* with the most variable coverage was the mapped dwelling foundation damage.

The approximate number of property observations used in the *damage attribute* datasets, which are correlated with the *calculated parameter* datasets are summarised in Table 8.1.

Table 8.1 Size of datasets used in this analysis

Earthquake	CPT	Number of properties with liquefaction observations	Number of properties with dwelling foundation observations	Number of properties with measurements of liquefaction related elevation changes
04 September 2010	5,500	22,400	8,200	39,500
22 February 2011	5,500	71,200	13,700	59,000
13 June 2011	5,500	70,000	37,300	70,500

8.3 Damage attribute quality

The limitations of the *damage attribute* datasets need to be understood before correlating them to the corresponding *calculated parameter* datasets. The reliability of the *damage attributes* is summarised in Table 8.2.

Table 8.2 Assessed reliability of damage attributes

Earthquake	Liquefaction observation attribute	Dwelling foundation damage attribute	Liquefaction related elevation change attribute
04 September 2010	High No previous damage existed	High Damage attribute is fresh	Low Based on comparison with 2003 LiDAR which had reduced coverage and slightly less accuracy. The LiDAR was flown the day after the September earthquake when ejecta was still present on the ground.
22 February 2011	High Mapping considered only new damage as September liquefaction cleared	Moderate Damage attribute can contain damage from September earthquake (which was typically smaller)	Moderate to high
13 June 2011	Moderate to high Mapping considered only new damage as February liquefaction cleared, but was only based on drive by inspections rather than individual property inspections	Low Damage attribute can contain damage that occurred in both September and February	Moderate to high

On the basis of this assessment, the liquefaction observation *damage attribute* is the most reliable parameter for primary comparison purposes. The liquefaction related elevation change observations are generally of good quality, but liquefaction related elevation change can occur due to mechanisms which are not just volumetric densification. The use of liquefaction related elevation change by itself does not represent all aspects of liquefaction related elevation change, especially lateral spreading. Liquefaction related elevation change is discussed in more detail in Section 9.3.3. The reliability of the dwelling foundation *damage attribute* reduces through the earthquake series and is not therefore as reliable for overall comparison purposes (refer to Section 3.2.2)

9 Damage attribute and calculated parameter comparison

9.1 General

This section presents a brief introduction to the data analyses that have been undertaken and provides some selected results. The *calculated parameter* datasets presented in this section are based on:

- (a) Data directly obtained from 5,500 CPT soundings and indirectly from 7,500 CPT soundings (Section 3.7)
- (b) Groundwater models from each main earthquake (Section 3.8)
- (c) PGA distributions from Cornell and UoC for each main earthquake (Section 3.4)

The scatter in the results is briefly discussed, followed by a discussion on the results obtained from a comparison of the *damage attributes* and *calculated parameters*. The data is presented in a series of appendices and summarised in Table 9.1 below. Information relating to the future performance of the land is presented in Section 10.

Table 9.1 Summary of appendices and data

Appendix	Data	Description
F	Main earthquakes maps	Maps of PGA, depth to groundwater, LPI, S and LSN plotted on top of liquefaction observation maps.
G	Main earthquakes graphs and analysis	Analyses showing land damage, foundation damage and liquefaction related ground surface subsidence correlated with LPI, S and LSN for the earthquake series.
H	Settlement maps (M6, M7.5)	Calculated settlement indicator mapped for a range of PGA values for M6 and M7.5 earthquakes based on a median groundwater depths to describe future land performance.
I	LSN Maps (M6, M7.5)	Calculated LSN mapped for a range of PGA values for M6 and M7.5 earthquakes based on a median groundwater depth to describe future land performance.
J	Settlement and LSN graphs and analysis	Data analyses of S and LSN based on TC2, TC3 and residential Red Zone areas to describe future land performance.

9.2 Scatter in datasets

A review of the datasets indicates that, while the correlation between the *damage attributes* and *calculated parameters* is clear and statistically significant, they contain a substantial amount of scatter. The majority of the scatter within the dataset correlations is attributed to possible variations in shaking intensity (PGA) and groundwater levels at the sites experienced at the sites compared with the modelled interpolated PGA values and groundwater levels. Other contributing factors resulting in potential scatter in the datasets include geological conditions, crust quality, lateral spreading superimposing damage from a different mechanism, the effect of liquefaction in the profile and the assumptions made regarding liquefaction triggering on a regional study basis. Each is discussed below.

Geological conditions

The geological conditions at sites are inferred based on nearby CPT. The Canterbury geological profile typically comprises interbedded alluvial deposits, which can vary substantially over short distances due to their deposition history. Accordingly, the interpolated *calculated parameters* inferred at sites may not be correlated directly to the geological profile that exists beneath the site.

We note that as the TC3 investigation continues to proceed, the resolution of the CPT investigation locations will improve and the scatter caused by interpolated *calculated parameters* will reduce. This will probably not be the case for TC2 areas where the number of additional CPT investigations are expected to be limited as part of the rebuild process.

Crust quality

The most reliable *damage attribute* has been assessed to be the volume of expressed liquefaction ejecta at the ground surface. The quality of the crust is inferred to affect the amount of liquefaction induced ejection that occurs. The crust quality is related to its soil properties (particle size distribution, plasticity, packing arrangement), consistency and number of penetrations (such as service trenches, power poles, foundations). These variables are not captured by the *calculated parameters* which therefore contribute to scatter in the dataset.

Variation between modelled and experienced PGA

The seismic loading at each site has been based on PGA models developed by Cornell and UoC. The actual seismic loading experienced at each site could vary locally due to local geological conditions or local seismic interference. Accordingly, the actual ground accelerations at sites is generally inferred rather than directly measured. Some *calculated parameters* are more sensitive to PGA compared to others.

For the assessment of future vulnerability described in Section 10, the level of seismic loading is not susceptible to uncertainty as it is based on a design shaking level.

Groundwater

The phreatic surface of the groundwater has been modelled to replicate groundwater conditions immediately prior to the 04 September 2010, 22 February and 13 June 2011 earthquakes. The groundwater model extends around urban Christchurch and represents the typical groundwater elevation. Very few monitoring wells were constructed prior to the earthquakes. Therefore, the earthquake specific groundwater models are based on inferring previous performance and contain uncertainty. The actual depth to groundwater at sites may have varied from the model.

For the assessment of future vulnerability described in Section 11, the groundwater assumptions have more certainty as around 800 monitoring wells have been installed and monitored across Canterbury. The median groundwater model surface is therefore based on directly measured data.

Probabilistic nature of liquefaction triggering

The liquefaction triggering processes are not presented as 'bright line' distinctions between sites affected or not affected by liquefaction. Moss et al. (2006) noted that a calculated factor of safety of 1.0 generally indicated a 15% chance of liquefaction affecting that soil layer. This probabilistic assessment means that some scatter will inherently be present in the generated data.

Lateral spreading

Some sites may have adequate crust thickness to mitigate the effects of differential settlement caused by the liquefaction of underlying soil layers which would be reflected in lower *calculated parameter values*. Therefore, if liquefaction occurs, these sites are theoretically not as vulnerable compared to sites with a thinner crust. However, if the land is sloping or near a free face (such as a water body), then there is the potential for lateral spreading to occur, increasing the damage at the site. This study does not consider or look at vulnerability damage due to the lateral spreading hazard. It was often difficult to distinguish between liquefaction induced damaging differential settlements and lateral spreading damage. Therefore, while sites may have low calculated liquefaction vulnerability parameters, they can be correlated with severe damage due to the lateral spreading hazard. This can cause scatter in the results. This is explained further in Section 12 and Appendix M.

Effect of liquefaction within the soil profile

The triggering correlations have been developed on the basis of the liquefaction of a single critical layer within the soil profile. In general, the soil profile with the lowest FoS can be expected to trigger first within the soil profile. Once liquefaction has occurred in the soil profile, the response of the soil profile to seismic shaking changes and therefore the likelihood of liquefaction changes. To model the sequence of liquefaction and the effect on various materials requires a detailed one-dimensional time-history shaking analysis that is not appropriate for this regional study, and is not used as standard engineering practice. This effect is noted and the potential to introduce scatter in the dataset is acknowledged.

Assumptions made to implement liquefaction triggering on a regional basis

A number of assumptions have been made to allow a regional analysis to be undertaken. These assumptions generally relate to aspects of analysis that could be addressed on an individual site basis, but are not able to be reasonably carried out for a regional dataset. The assumptions include

- (a) *I_c* cut off
The assumption that the risk of liquefaction is negligible above a certain *I_c* value
- (b) Fines content
Estimation of fines content based on the CPT results
- (c) Pre-drill
The interpolation of the nature of pre-drilled parts of the CPT profile based on nearby CPT
- (d) Thin layer/transition zone assessment
The effects of thin layers and transition between material types can be considered on an individual basis, but cannot be reasonably automated for a regional study

9.3 Primary dataset results

9.3.1 General

A visual inspection of the *primary datasets* has been carried out and is presented below. The inspection compares the *calculated parameters* LPI, *S* and LSN with the *damage attributes* land and dwelling damage and liquefaction related elevation change. Box and whisker plots and cumulative frequency graphs correlating the *damage attributes* and *calculated parameters* are presented in Appendix G and discussed below. Both the Cornell and UoC PGA distributions are considered.

9.3.2 Liquefaction Potential Index (LPI)

Land damage

The correlation between LPI and land damage within earthquakes shows a trend of generally increasing damage with increasing LPI. While the results for individual earthquakes show good correlations, the slope of the correlations vary for each earthquake. This characteristic is particularly marked in the 22 February 2011 results. The ability of LPI to differentiate between land damage categories is limited. The UoC and Cornell PGA distributions results show generally consistent trends, but have variations in values.

The range of typical LPI for damage is presented in Section 5.2. LPI values of less than 5 indicate a low risk of liquefaction, while an LPI of more than 15 indicates a very high risk of liquefaction. The data shown in the figures is inconsistent with the published ranges. A significant proportion of sites with very little damage have an LPI of more than 5, while a number have severe damage but an LPI of less than 5.

Dwelling foundation damage

The relationship between dwelling foundation damage and LPI is poor. The ability of LPI to differentiate between damage classes is low. The consistency of LPI between earthquakes is not

strong, with variations in LPI for each of the damage classes. There is a broad agreement in trends with both the UoC and Cornell PGA distributions, although the values do vary between the two models.

Liquefaction related elevation change

The LPI is a poor predictor of liquefaction related elevation change, with little differentiation between measured elevation changes. The correlation between the liquefaction related elevation change and the calculated settlement indicator is poor, varies between earthquakes, and also depends on the PGA distribution used.

9.3.3 Calculated settlement indicator (S)

Land damage

The graphs show a generally increasing trend between the calculated settlement indicator and the land damage for the land damage category. There is a substantial overlap between the *calculated parameters* for the earthquakes, with only weak trends observed. The calculated settlement does not have strong repeatability across earthquakes, but is consistent between the two PGA distributions considered.

Dwelling foundation damage

The calculated settlement indicator shows a weak trend with the dwelling foundation damage category. There is poor differentiation between damage categories and the repeatability between earthquakes is low. The consistency in calculated values based on the UoC and Cornell PGA distributions is high.

Relationship between the calculated settlement indicator and the liquefaction related elevation change

Box and whisker plots of the volumetric densification calculated settlement indicator have been compared to the LiDAR measured liquefaction related elevation changes for three main earthquakes. The measured liquefaction related elevation changes are tectonically adjusted (i.e. are corrected for the regional deformations caused by the earthquakes).

Overall, the correlation between the LiDAR measured liquefaction related elevation changes and the calculated volumetric densification settlements is assessed as weak for all earthquakes.

Figures showing individual points for the measured settlements are presented in Figures G4 and G5. These show that there is little to no correlation between the calculated settlement indicator and liquefaction induced elevation changes. There are a number of possible explanations for this including

1. Ejection of liquefied material

The calculated settlement is based on empirical correlations of volumetric strain that do not consider the contribution of liquefied material being ejected to the ground surface. This mechanism was widespread around Canterbury. The presence of this mechanism should theoretically result in higher liquefaction related elevation changes than calculated settlements.

2. Lateral spread

When ground spreads laterally into a waterway it subsides. Properties that experienced this damage mechanism are included in the dataset, but this is not considered in the volumetric densification calculation. This mechanism should result in higher liquefaction related elevation changes compared to calculated settlements.

3. Repeated liquefaction

The laboratory tests on which the empirical volumetric densification correlations were carried out were based on volumetric densification under cyclic shear strains. If the materials do indeed densify, then the relative density of the materials must increase. This means that amount of subsequent volumetric densification under further cyclic shearing should reduce as the material densifies. This mechanism is not considered in the calculation.

On the basis of the reasons stated above, and given the variation in the calculated and measured liquefaction related elevation changes at sites, the figures show that the correlation between calculated settlement and liquefaction related elevation change is poor.

It is important to re-emphasise that the calculated settlement indicator based on volumetric densification correlations better represents a proxy for liquefaction related damage at the ground surface for the soils in Canterbury rather than acting as a predictive tool for calculating liquefaction related elevation change.

9.3.4 Liquefaction Severity Number (LSN)

Land damage

There is a reasonably good correlation between LSN and the land damage for all of the earthquakes and PGA distributions considered and the correlations are reasonably similar for each earthquake. The LSN provides a differentiation between the various categories of land damage for various LSN, with relatively small changes between earthquakes. There is general consistency in the LSN results for each of the damage classes.

Dwelling foundation damage

LSN has a weak relationship with the dwelling foundation damage attribute. There is a consistent, albeit weaker, trend of increasing damage with LSN through all scenarios. There is little difference between the UoC and Cornell PGA distributions.

Liquefaction related elevation change

The measured liquefaction related elevation change exhibits a weak to very weak correlation with LSN. The LSN has significant overlap and is a poor predictor of liquefaction related elevation change, with some scenarios showing reductions in elevation change with increasing LSN.

9.3.5 Maps

Maps of the *calculated parameters* have been prepared and are presented in Appendix F. The maps show the spatial distribution of the various *calculated parameters* overlying the mapped liquefaction and lateral spreading observations. In the areas where the soil has lower thicknesses of material with an $I_c > 2.6$ in the upper 10 m, the results are generally consistent with the observed land damage around the region. However, the following areas are identified as having systemic differences. These are discussed below.

Southeastern Christchurch

The southeastern area of Christchurch consistently calculated higher *calculated parameters* than the observed damage. The locations of strong motion recording stations in Christchurch are shown on the PGA maps in Appendix F. The figures show that the southeastern area of

Christchurch has very few strong ground motion sites, and that the ground acceleration distributions for this area are strongly influenced by the Heathcote Valley School seismograph station (HVSC). The station has consistently recorded higher accelerations than other sites subjected to similar ground motions. Bradley (2012c) noted that this site could be affected by basin edge effects and be on different soil conditions to sites on the flat alluvial deposits of Canterbury. Observations of the site and area indicate that this is likely to be a reasonable explanation for the observed high loading that does not match with the observed damage, resulting in higher calculated LPI, S and LSN parameters.

Southwestern Christchurch

The southwestern area of Christchurch consistently calculated higher *calculated parameters* than observed damage. This area is characterised by the relatively high thickness of high fines content material and a groundwater table closer to the ground surface. Figures 43 and 44 in Appendix A show that this area has a higher proportion of fine grained material (with $I_c > 2.6$) than is typical around Canterbury. The area is shown on Figures C1 to C14 to be of relatively low elevation and known around Christchurch as being 'swamp-like', with weak materials at or near the ground surface and a shallow groundwater table (refer to the maps in Appendix C).

In the assessments, fine grained material with $I_c < 2.6$ is assumed by the CPT triggering methods to be susceptible to liquefaction and hence make a full contribution to the *calculated parameters*. In practice, however, soils with I_c materials close to 2.6 are in fact less likely to be susceptible to liquefaction than soils with significantly lower I_c values and the analysis may therefore be conservative. In addition, it is likely that the swampy nature of the material and the presence of more finer grained materials means that the expression of liquefaction and the effects at the surface will be mitigated. The *calculated parameters* in this area are therefore inferred to over-estimate the actual observed damage due to the high fines contents in this area.

Avon River and adjacent suburbs

The correlation between the *calculated parameters* and the mapped damage is very strong along the Avon River and nearby. In general, the *calculated parameters* provide a generally good fit to the data observed around the Avon River, particularly in areas away from areas affected by lateral spreading. However, in Avonside the *calculated parameters* were low but experienced significant damage. This is discussed more in Section 12, but is attributed to lateral spreading cracking the crust and allowing the effects of liquefaction to become more severe.

9.4 Conclusions

The *calculated parameters* have been compared with *damage attributes* for the main earthquakes of the Canterbury Earthquake series. The results have been presented in this section and are summarised in Table 9.2 below. Of the three *calculated parameters* considered, the LSN provides the best, most repeatable indicator of vulnerability to liquefaction.

The MBIE guidance recommends that a settlement index be calculated for foundation design purposes. Therefore, on the basis of the correlated damage, both LSN and the calculated settlement indicator will be considered for the future predictions considered in Section 11.

Table 9.2 Summary of quality of dataset correlations

	LPI	Calculated settlement indicator	LSN
Differentiation of land damage attribute	Moderate	Low	Moderate to high
Consistency between earthquakes	Low to moderate	Low to moderate	Moderate to high
Consistency between UoC and Cornell PGA distributions	Moderate to high	Moderate	Moderate to high
Ability to respond to change in crust thickness	Moderate	Very low	High
Overall performance of the calculated parameter to predict liquefaction related damage	Moderate	Low	Moderate to high

10 Study of additional earthquakes

10.1 General

This section presents the results of the application of LSN to other earthquakes that have occurred during the Canterbury Earthquake series where ground surface manifestation of liquefaction was observed. Most of these earthquakes were generally much closer to the residential 'serviceability limit state' (SLS) design earthquake (1 in 25 year return period) for residential dwellings than the three main earthquakes.

As these were relatively small earthquakes that caused localised damage, they did not receive the same detailed level of land observations mapping as the main earthquakes. PGA contours for the earthquakes have been prepared by Cornell and UoC. The groundwater models and extent of damage mapping carried out for each of the earthquakes is summarised in Table 10.1 below.

The results of the calculations for the earthquakes listed in Table 10.1 are presented in Appendix F. Each of the smaller earthquakes is discussed in separate subsections below.

Table 10.1 Summary of earthquakes analysed

Earthquake	Groundwater model	Land damage attribute mapping
04 September 2010 ¹	Modelled for earthquake	Mapped on house by house basis
22 February 2011 ¹	Modelled for earthquake	Mapped on house by house basis
16 April 2011	Based on June 2011 ²	See s10.2
13 June 2011 (Event A)	Modelled for earthquake	See s10.3
13 June 2011 (Event A and B) ¹	Modelled for earthquake	Mapped on road by road basis
23 December 2011 (Event A and B)	Modelled for earthquake	See s10.4

Notes: ¹ denotes the main earthquakes for which detailed analyses have been undertaken (refer Sections 3.8,9,10 and Appendix E in this report)

² the 13 June 2011 groundwater depths are assumed to be applicable for the 16 April 2011 earthquake.

10.2 Earthquake comparison – 16 April 2011

Maps associated with this earthquake are presented as Figures F19 to F27. GeoNet recorded a magnitude 5.3 earthquake at 5:49pm on 16 April 2011. It was centred at a depth of 11 km and around 20 km southeast of Christchurch. A geotechnical engineer made observations of the general areas where sand ejection had occurred at the ground surface on the afternoon of 17 April 2011. These general observations are summarised on Figure A5.

The LSN map shows the highest LSN in the southeastern corner of the city. As discussed in Section 9.3.5, we expect that this is due to the influence of the Heathcote Valley recording station results in higher PGA modelled around that site than was actually experienced. The other areas with higher calculated LSN are located in the general areas where liquefaction was observed. There is a reasonable correlation between LSN and observed damage, although we note that Bexley did not generate high LSN despite liquefaction damage being observed in the area. The settlement map does not identify the damage observed adjacent to the Avon River.

10.3 Earthquake comparison – 13 June 2011 (Event A)

Maps associated with this earthquake are presented as Figures F28 to F36. GeoNet recorded a magnitude 5.6 earthquake at 1:01pm on 13 June 2011. Note that the earthquake magnitude calculated by GeoNet differs to that analysed and calculated by others. The earthquake was centred at a depth of 6 km and around 10 km east of Christchurch. This earthquake was the first of two main earthquakes that occurred that afternoon, with a second at 2:20pm. A drive-by inspection was being carried out by geotechnical engineers and general areas with sand ejection due to the first earthquake were being noted on the maps when the second earthquake occurred. The extent of the observations that had been made when the second quake occurred is shown on Figure A6.

The LSN maps show high calculated LSN values in southwestern and southeastern Christchurch and along and adjacent to the banks of the Avon River. The reason for high values in these areas has been discussed in Section 9.3.5. The remainder of the map shows calculated LSN values that tend to be more severe than the observed liquefaction severity attributes noted on the map. This systemic overprediction of the LSN parameter may possibly be due to the groundwater model being closer to the ground surface than was actually the case as well as the larger magnitude earthquake being modelled. Despite the higher LSN, the maps show that there is a moderate to strong correlation between the calculated LSN and observed damage for the areas inspected.

The calculated settlement indicator map shows areas similar trends to LSN having higher values than the surrounding areas. However, these calculated settlements are low in magnitude and do not provide good quality differentiation between damaged and non-damaged areas. Higher settlements were again calculated through southwestern and southeastern Christchurch (discussed above).

10.4 Earthquake comparison – 23 December 2011 (Event A and B combined)

Maps associated with this earthquake are presented as Figures F46 to F54. GeoNet recorded an earthquake at 3:18pm on 23 December 2011. It was centred at a depth of 6 km and around 10 km east of Christchurch. This earthquake was the second of two main earthquakes that occurred that afternoon. The earthquake occurred the afternoon of Friday before Christmas, and limited staff were available to carry out detailed property by property observation mapping. Accordingly, inspection results from drive by inspections are presented.

The LSN maps show a generally good correlation, with notable liquefaction damage generally observed in areas of high LSN. The major discrepancies identified occur in the southern area of Christchurch, which has been discussed in Section 9.3.5.

The calculated settlement indicator map does not provide as good a correlation with observed land damage compared with the LSN maps. In particular, areas along the Avon that suffered severe liquefaction were not clearly identified in the calculated settlement map.

11 Future performance

11.1 General

The previous sections of this report have presented the results of back analysis of vulnerability indicators in Christchurch based on the earthquakes that have occurred and the damage observations that have been made. This section presents the results of analyses, where the performance of areas of Christchurch are considered on the basis of varying seismic design earthquake loadings for the median groundwater scenario. The calculated settlement indicator and LSN are compared and discussed, and maps and graphs showing the results are presented in Appendix H, I, and J.

The inputs to the modelling are briefly presented, followed by a discussion of the results.

11.2 Primary dataset analysis

11.2.1 Inputs

To assess the future vulnerability of land at specific design return period levels of seismic load requires an assessment of the geological profile, the seismic loading and an assumed groundwater regime. Each of these is briefly discussed below.

Geological profile

The geological profile here is represented by CPT at discrete locations. The dataset interpolates between CPT and so may not capture the natural variability of soil deposits. The dataset construction process is discussed in more detail in Section 8.

Seismic loading

A range of seismic loading values have been modelled, ranging from 0.08g to 0.40g. The range of values allows the response of the ground to be considered over a range of ground acceleration scenarios including the current residential SLS and ULS levels of loading at 0.13g and 0.35g respectively. Both a M6.0 and M7.5 earthquake have been modelled to represent the response to different earthquake scenarios that could occur in Canterbury.

Groundwater

Groundwater levels around Christchurch have been recorded to vary seasonally and inter-annually (van Ballegooy et al. 2013). Some parts are more controlled by local rainfall recharge (elevating groundwater in the winter period) and others are more controlled by the groundwater flow from water infiltration in the Southern Alps (generally elevating groundwater in the spring period and following snow melt). Other areas closer to the coast or rivers are more controlled by sea level and tend to have less seasonal and inter-annual fluctuations.

A median groundwater table has been presented in van Ballegooy et al. (2013) and this has been used for the prediction of liquefaction vulnerability for future seismic loading. Groundwater levels for future seismic loadings have been modelled using the median groundwater surface. The adoption of a median groundwater table is consistent with the probabilistic seismic hazard modelling. The seismic hazard at SLS or ULS represents a probability of a hazard occurring. The median groundwater table is the mid-point between summer and winter conditions and represents the 50th percentile groundwater elevation. This means that there is a 50% chance that the actual groundwater elevation is higher, and a 50% chance that the groundwater elevation is lower. If a groundwater surface was adopted that was only exceeded for two months of the year (an 85% condition), then the analysed hazard probability calculation would be representative of a longer return period seismic load.

The median groundwater model has been combined with the most recent (post-December 2011) LiDAR data. No major earthquakes have occurred since the LiDAR survey was undertaken and hence this ground surface elevation model is applicable.

11.2.2 Results

The results of the analyses are presented graphically as maps in Appendix H and I. Appendix H contains maps showing the calculated settlement indicator, while Appendix I presents the same maps showing the calculated LSN. The results have been correlated against the TC2, TC3 and residential Red Zone properties and plotted as box and whisker plots, cumulative frequency plots and *calculated parameters* and PGA response curves in Appendix J. The graphs are presented for both M6.0 and M7.5 earthquake PGA.

The graphs show that neither settlement nor LSN provide clear differentiation between TC2 and TC3 properties, particularly at lower PGA. LSN differentiates the residential Red Zone from TC2 and TC3 properties for most PGA levels, whereas calculated settlement does not provide as strong a differentiation.

As expected, the initiation of liquefaction and hence calculated settlement indicator and LSN is delayed for the M6.0 analyses compared with the M7.5 analyses. The M6.0 earthquakes represent smaller, more local earthquakes (near field, like the 22 February 2011 earthquake), while the M7.5 represents larger earthquakes that are likely to occur further away from the city (far field, like the 04 September 2010 earthquake). The 04 September 2010 earthquake comprised a M7.1 around 40 km from the city, while the 22 February 2011 earthquake was M6.2 around 5 km from the city centre. It is noted that the maps in Appendix H and I are based on an assumed constant level of seismic shaking across the city. Actual distributions of seismic loading will vary spatially which would in turn modify the *calculated parameters*.

The figures, tables and graphs show that the calculated settlement indicator has substantially more overlap between the TC2 and TC3 properties compared with residential Red Zone properties. The LSN parameter clearly distinguishes residential Red Zone from TC2/TC3 properties at all levels of shaking above 0.13g. The calculated settlement indicator shows a trend of increasing predicted damage with increasing settlement, and there is substantial overlap between TC2, TC3 and Red Zone areas. The LSN differentiates between TC2/TC3 and Red Zone more clearly, with very little overlap between TC2 and Red Zone. TC2 and TC3 properties were observed to perform similarly in the 04 September 2010 earthquake, and so overlap of these categories is consistent with these observations.

The number and nature of CPT in each of the technical categories varies. The CPT in TC2 were typically pushed during an early stage of the investigation where pre-digging of CPT locations was taking place. More than 60% of the TC2 CPT have been pre-dug, compared to 10% of CPT in TC3. The pre-digging removes information from the record. Interpolation from nearby CPT (including

CPT < 5 m depth) has been carried out where possible, but the density of CPT in TC2 areas generally does not make this feasible. For this regional study, parameters representing materials highly susceptible to liquefaction have been adopted. This assumption appears to be altering the response of the TC2 areas, probably by over-predicting LSN. Further analysis could be undertaken if more CPT in TC2 areas become available.

11.3 Observed liquefaction at 100 year return period seismic loading

The performance of land due to approximately 100 year return period seismic loading has been assessed. The 100 year return period seismic loading under current design criteria is around 0.2g for a M7.5 earthquake. The PGA distribution produced by UoC for the main earthquakes have been magnitude weighted to an equivalent M7.5 earthquake using the method presented in Idriss & Boulanger(2008). The areas with magnitude weighted PGA between 0.15g and 0.25g have been isolated for each of the earthquakes and are presented on Figure K1.

Liquefaction related land damage has been identified at sites based on the mapping carried out, supplemented by aerial photographs and additional data sources. These have been used to identify the number of times that liquefaction around the 100 year return period seismic loading manifested at the ground surface at each site. The comparison is used to classify the vulnerability of properties in these areas to the approximately 100 year return period seismic loading. The classification of these properties is shown on Figure K2.

Analysis has been carried out on the response of properties identified on Figure K2. The calculated settlement indicator and LSN have been calculated for these properties over a range of PGA in a similar manner to the analysis grouped for the different Technical Category presented in Section 11.2. The analysis results are similar to those of TC2 and TC3 discussed in Section 11.2.

The calculated settlement indicator has higher variability than the LSN. The LSN shows better separation between vulnerable and non-vulnerable land than the calculated settlement indicator. In most cases the differentiation between vulnerable and non-vulnerable areas is stronger than that between TC2 and TC3 zones, and this is particularly evident at higher PGA values.

There is general agreement between vulnerable areas identified based on field observations of damage and *calculated parameters* based on site investigation data. This consistency shows there is robustness within the classification process. Areas that are vulnerable around the 100 year earthquake seismic load can be identified either by site observations after an earthquake or by site investigation and testing prior to an earthquake occurring.

11.4 Sensitivity to groundwater

Appendix L shows the effect of increasing and decreasing the depth to groundwater by 20%. The calculated settlement indicator and LSN are presented for M7.5 PGA of 0.13g, 0.22g and 0.35g. These are followed by graphs showing the change in response of the parameters in the various technical categories.

The analyses show that LSN responds significantly to groundwater level change, which affects the thickness of the upper crust of non-liquefiable materials. The literature review (Section 5) noted that crust thickness had an influence on surface effects, and this is generally confirmed by these observations. The settlement based analyses do not respond the same way to the different groundwater models, with little change between the elevated and reduced groundwater conditions. In general, the LSN maps identify the areas most affected by liquefaction damage, particularly at lower (SLS or similar) levels of seismic loading.

12 LSN and lateral spread

An area within the Avonside loop has been assessed in more detail to provide a local micro-study on the effects of lateral spreading on land damage and its correlation with the *calculated parameters*. The area selected has had a number of CPT soundings carried out, both around the perimeter and within the centre of the loop. The location and extent of the study area is restricted to the loop of the Avon River surrounding Avonside and generally north of Morris Street.

The study area was selected as it was subjected to severe lateral spreading and contained sites that experienced severe land and dwelling foundation damage. The figures listed in Table 12.1 show the study area with the mapped *damage attributes* and *calculated parameters*.

Table 12.1 Summary of figures in Appendix M for study area Avonside

Figure number	Title Commentary
M1	Dwelling foundation damage attribute (worst observed)
M2-M5	LiDAR Elevations pre-September 2010, post-September 2010, post-February 2011 and post-June 2011.
M6-M8	Change in LiDAR elevations with LSN overlaid pre to post-September 2010, pre to post-February 2011, pre to post-June 2011
M9—M11	Mapped land damage with LSN overlaid Post-September 2010, post-February 2011 and post-June 2011.
M12-M13	Vectors – not tectonically adjusted Vectors –resultant (tectonically adjusted) pre to post-September 2010, pre to post-February 2011, pre to post-June 2011

The results are discussed below.

LiDAR elevation

The LiDAR data shows that the centre of the loop has settled during the earthquake series. The most substantial drop is due to the 22 February 2011 earthquake. The edges of the loop that were observed to have been most affected by lateral spreading have settled significantly.

04 September 2010 earthquake

The LSN map for the 04 September 2010 earthquake shows that the perimeter of the Avonside loop is assessed to have very high LSN and to be at risk of severe damage. The land damage mapping carried out indicates that the northeastern perimeter experienced severe damage, but that the amount of damage reduced towards the southwest. The centre of the area typically had low LSN calculated, but had moderate amounts of material ejected.

The vector maps and crack maps show that there was a significant amount of stretching and cracking in the centre of the loop due to lateral spreading, which would have created pathways for the liquefied material to eject through to the ground surface. Therefore, the prediction of low vulnerability to the liquefaction hazard in the centre area may not be unreasonable because the damage was caused by the lateral spreading hazard. If perimeter treatment work to mitigate the lateral spreading hazard had been in place prior to the earthquakes, then it is likely that the centre of the Avonside loop area may have experienced little to no liquefaction damage given the centre area has a greater non liquefying crust thickness compared with the perimeter.

22 February 2011 earthquake

The post 22 February 2011 LSN is generally higher than that calculated for the 04 September 2010 earthquake, consistent with the land performance observations.

13 June 2011 earthquake

The LSN calculated for the 13 June earthquake are the highest of the three earthquakes considered. The high LSN extends almost to the centre of the study area. The mapped land damage indicates that the area was severely affected by liquefaction, with the entire loop indicating moderate to severe liquefaction and lateral spreading land damage. The increased LSN values are mainly due to higher groundwater levels and because the land has subsided due to damage from the 04 September 2010 and 22 February 2011 earthquakes.

Dwelling foundation damage

The map of dwelling foundation damage shows that the perimeter was affected substantially more than the interior part of the loop.

Summary and conclusion

The LSN and land damage discrepancies within the Avon loop area considered in this micro study are explained by the presence of lateral spreading. LSN provides a good prediction of areas likely to be affected by liquefaction damage at the ground surface, but does not correlate well with the areas where there is a thicker crust and where the land is susceptible to lateral spreading. In these areas the predominant cause of damage is due to lateral spreading. Therefore, the match between the calculated LSN values and observed damage is good if damage caused by lateral spreading effects are isolated and removed.

13 Examples of LSN

Photographs have been collated showing the distribution of observed land damage for selected LSN ranges (e.g. LSN of 0-10, 10-20 etc.). A summary of these photos is presented on Figures A48 and A49, with the full photo set presented in Appendix N. The figures show that there is a clear and consistent trend that sites with higher LSN values experience more severe land damage than sites with lower LSN values.

The typical behaviour of sites with a given LSN are summarised in Table 13.1 below. It is important to reiterate that the LSN describes a range of possible damage and the information below represents only a typical behaviour. The actual site performance may sometimes vary from this.

Table 13.1 LSN Ranges and observed land effects

LSN Range	Predominant performance	Photographs in Appendix N
0 – 10	Little to no expression of liquefaction, minor effects	Figure N7a-y
10 – 20	Minor expression of liquefaction, some sand boils	Figure N8a-y
20 – 30	Moderate expression of liquefaction, with sand boils and some structural damage	Figure N9a-t
30 – 40	Moderate to severe expression of liquefaction, settlement can cause structural damage	Figure N10a-v
40 – 50	Major expression of liquefaction, undulations and damage to ground surface, severe total and differential settlement of structures	Figure N11a-p
>50	Severe damage, extensive evidence of liquefaction at surface, severe total and differential settlements affecting structures, damage to services.	Figure N12a-x

14 Discussion

This report has considered the three liquefaction vulnerability indicators of LPI, S and LSN and their relationship with liquefaction induced damage in Canterbury in the recent earthquakes. The indicators have been calculated and compared to observations of land damage, dwelling damage and liquefaction related elevation change. These comparisons are discussed below and it is concluded that LSN provided a good quality tool to correlate land damage. An analysis of the effect of future possible seismic loading was then undertaken for LSN and the calculated settlement indicator.

The majority of research work that has been carried out relating to liquefaction has focussed extensively on the susceptibility of soil materials to liquefaction. Some studies have addressed the consequences of liquefaction. The assessments of the effects of liquefaction are generally based on a limited number of case studies at selected sites. Examples of this are noted in the Ishihara (1985) and Youd and Garris (1995) studies on the effect on crust thickness. The nature and response of individual sites can be carefully assessed and used to guide recommendations on consequences. This approach benefits from the level of knowledge of individual sites, but can make the development of trends from the data difficult.

The Canterbury earthquakes have provided a unique opportunity to undertake a regional assessment of the effects of liquefaction on residential dwellings. The analyses carried out and reported here are only possible due to the relatively high level of information relating to:

- (a) The ground acceleration distribution through the earthquake series based on numerous strong ground motion stations
- (b) The geological profile through areas affected by liquefaction assessed by CPT
- (c) A well developed groundwater model with an understanding of the variability both seasonally and through the earthquake series
- (d) Mapping of the severity of land damage after each of the main earthquakes
- (e) Mapping of dwelling foundation damage at around 75,000 properties
- (f) LiDAR data showing ground settlements, adjusted for tectonic effects

This data can be combined into large datasets and used to extract trends in the data. It should be noted that this regional analysis introduces a different kind of error to site specific analyses, with trends able to be extracted from the population, but variation in the performance of individual sites readily identifiable. There is inherent variability in the generated datasets, and this is attributed to the interpolation that is carried out, the inherent probabilistic nature of liquefaction analysis and the effect of non-modelled variables such as crust quality. The variability of the datasets is likely to reduce as additional CPT are pushed.

None of the parameters considered in this report are intended to consider the risk of lateral spreading affecting sites. Lateral spread is caused by liquefaction in conjunction with surface geometry and falls outside the scope of this document.

Groundwater

The groundwater modelling provides an assessment of the groundwater conditions in the subject area at the time of each earthquake. The median groundwater table has been calculated based on historical data. Liquefaction effects are sensitive to the crust thickness, which is often directly related to the depth to groundwater. Groundwater modelling is therefore an important aspect of the analysis.

The depth to groundwater varies across the city and generally increases towards the west. The eastern suburbs that were most affected by liquefaction related effects often had very shallow groundwater depths.

Liquefaction triggering

The liquefaction triggering method adopted in this analysis is that presented in Idriss & Boulanger (2008). Other liquefaction triggering methods were considered in analyses reported under a separate cover. The specific analysis used did not make significant differences to the results. While the methods considered provided generally consistent results, there are advantages in selecting a single method that ensures repeatability and consistency in the analyses carried out. The Idriss and Boulanger method was selected as the most recent method that also generally provided the lowest variation and best differentiation in the data comparisons.

Crust thickness

The work of Ishihara (1985) and then Youd and Garris (1995) captures the importance of crust thickness in providing protection from liquefaction effects at the ground surface. This proposed relationship between crust thickness and land damage was shown in the results discussed in Section 5 and confirmed by observations of liquefaction effects around Canterbury during the earthquake series. The parameters that represent vulnerability of the land should represent the effect that changing crust thickness has on vulnerability.

Calculated parameters – discussion

LPI

The LPI provides a good indication of the risk of the severity of liquefaction occurring at the site. It weights the depth of liquefaction and has the ability to respond to increasing peak ground accelerations. However, it is relatively insensitive to crust thinning effects. While LPI provides a good correlation with land damage within an earthquake, the LPI range associated with each damage category tends to vary between earthquakes. This behaviour makes it less useful when considering the vulnerability of sites under possible earthquake scenarios.

The LPI is based on a weighted function of '1-FoS'. As the FoS drops, the LPI therefore increases. This increase continues with increasing seismic loading. As a result, the LPI does not tend to 'plateau'.

When the smaller earthquakes were considered, the LPI was not a good indicator of areas that showed evidence of land damage.

Calculated settlement indicator

The regulatory framework assessments of liquefaction vulnerability (MBIE, 2012) are based on an indexed settlement indicator. The quality of this parameter has been tested by comparing it with the observed *damage attributes*. There is a strong correlation between the calculated settlement parameter and the risk of liquefaction occurring at a site. The parameter increases with the depth of the CPT, but is insensitive to reducing crust thickness. This lack of sensitivity to crust thickness is inherent in this parameter, as no weighting is given to the depth at which liquefaction occurs. The calculated settlement indicator is a good indicator of risk of liquefaction affecting a site, but does not clearly differentiate between the level of damage experienced.

The calculated settlement indicator is based on correlations presented by Zhang et al. (2002). These correlations relate the calculated FoS against liquefaction with the volumetric strain, depending on the relative density of the material. The relative density is determined by the CPT tip resistance. The correlations consider factors of safety less than 2, which tend to reach a maximum volumetric densification strain at factors of safety around 0.6 to 0.7. Where the FoS drops below this, the volumetric strain does not tend to increase. The settlements therefore tend to approach a maximum value at a certain seismic loading, above which the calculated settlement indicator does not tend to increase significantly.

When the smaller earthquakes (discussed in Section 10) were considered, the calculated settlement index was not a good indicator of areas that showed evidence of land damage.

LSN

LSN provides a strong correlation with land damage that is generally consistent between earthquakes. It heavily weights liquefaction in upper materials more than deeper materials and therefore has the ability to respond strongly to changes in the crust thickness.

By way of comparison, LPI weights liquefaction at a depth with a linearly reducing function from 0 to 20 m, while LSN weights depth with a hyperbolic function ($1/z$). LSN represents the severity of liquefaction using the volumetric strain presented in Zhang et al. (2002). This strain calculation self-limits the proxy for severity of liquefaction depending on the relative density of the material. The LSN therefore tends to plateau in a manner similar to that for the calculated settlement indicator discussed above.

When the smaller earthquakes were considered, the LSN was the most sensitive parameter to indicating the onset of liquefaction related damage at the ground surface. It provides a suitable tool for assessing liquefaction vulnerability at both low and high PGA.

General

Of the three parameters considered, LSN provides the strongest correlation with land damage. The land damage correlations do contain scatter, but clear conclusions can still be drawn relating to the quality of the correlation. Of the parameters considered, LSN is assessed as the most suitable as it

- (e) Is generally best at differentiating the severity of observed land damage
- (f) Is generally more consistent between earthquakes with respect to this differentiation
- (g) Is the most responsive to the effects of reducing crust thickness

The quality of LSN correlation with dwelling damage can be seen in Appendix N, where the foundation damage has a weaker relationship with LSN.

A review of the maps, box and whisker plots and cumulative frequency graphs shows that there is scatter in all of the parameters considered. This scatter is inherent in the regional study that is undertaken. Despite this scatter, the typical land damage associated with LSN ranges is demonstrated in photographs attached in Appendix N.

Areas in the southeast and southwest have been identified on the maps that have systematic discrepancies between the *calculated parameters* and the observed land damage. These areas typically calculate a high *calculated parameter* relative to the severity of the observed liquefaction land damage. This over prediction has been attributed to the fines content and possible effect of the Heathcote Valley School ground acceleration records and was discussed Section 9.3.5.

Land has been identified that has experienced seismic loading around 0.2g (generally relating to the 100 year return period earthquake). The degree of vulnerability of land subjected to this seismic loading was assessed by comparing the number of times that it was loaded with the number of times that liquefaction was observed. Analyses were carried out on these sites to assess how the LSN and calculated settlement indicator respond to various seismic loads. The response is similar to that observed for the main dataset analysis considering TC2 and TC3 properties, LSN providing better differentiation between sites with severe liquefaction vulnerability and sites with lower liquefaction vulnerability. The calculated settlement parameter showed a trend of increasing damage but had more overlap between severe and less severely damaged properties.

There is general agreement between vulnerable areas identified based on field observations of damage and *calculated parameters* based on site investigation data. This consistency shows there is robustness within the classification process. Areas that are vulnerable around the 100 year earthquake seismic load can be identified either by site observations after an earthquake or by site investigation and testing prior to an earthquake occurring.

15 Summary and conclusions

This section presents a brief summary of the analyses carried out and conclusions relating to the liquefaction vulnerability study. This section contains a summary of selected points and the reader is directed to the text in the report for the detail related to the various aspects of this study.

1. This report evaluates different indicators that can be used to characterise land vulnerability to the liquefaction hazard for residential properties affected by the Canterbury earthquake series. The evaluation relies on the comparison of measured *damage attributes* (observations) and *calculated parameters* (vulnerability indicators) based on the geotechnical investigation data.
2. The *damage attribute* datasets that have been collected represent liquefaction effects on properties and comprise:
 - a. Liquefaction and lateral spreading observations (based on observations made after each significant earthquake)
 - b. Observed dwelling foundation damage
 - c. Liquefaction related elevation changes (derived from flown LiDAR surveys)
3. Three *calculated parameters* have been considered and compared with the measured *damage attributes*. These *calculated parameters* comprise
 - a. Liquefaction Potential Index (LPI)
 - b. Calculated settlement indicator (S)
 - c. Liquefaction Severity Number (LSN)
4. The *calculated parameters* have been calculated for 7,500 CPT available in the Canterbury Geotechnical Database using the following methods:
 - a. LPI, using the Idriss & Boulanger (2008) liquefaction triggering method
 - b. S, using the Idriss & Boulanger (2008) liquefaction triggering method and Zhang et al. (2002) volumetric densification correlations.
 - c. LSN, using the Zhang et al. (2002) volumetric densification method and Idriss & Boulanger (2008) liquefaction triggering method.
5. The *calculated parameters* are based on the spatial distributions of peak ground acceleration prepared by researchers at University of Canterbury and Cornell University.
6. *Damage attributes* from the earthquakes have been compared to the *calculated parameters* of settlement and LSN as a primary data analysis.
7. Groundwater models representing pore water pressure conditions that existed immediately prior to each earthquake and have been used for the calculation of the *calculated parameters*.
8. For this regional study, liquefaction has been assumed not to occur where the soil behaviour type classification index I_c exceeds 2.6. This is generally consistent with published recommendations by Robertson & Wride (1998). The Idriss and Boulanger (2008) liquefaction triggering method has used an automated assessment of the apparent fines content based on the Robertson and Wride (1998) method.
9. For each of the earthquakes the non-liquefying crust thickness and the cumulative thickness of liquefying material have been addressed at each CPT location. The results were superimposed onto a Youd and Garris (1995) plot of the Ishihara criteria, divided into sites where liquefaction was observed and sites where liquefaction was not observed. The plot does not separate the datasets showing that the Ishihara criteria are not suitable for Christchurch. This is attributed to other variables that affect site performance.
10. A visual inspection of maps for the datasets shows that the majority of the areas most affected by liquefaction coincide with low lying areas where the ground water table is shallow. Conversely, sites less affected by liquefaction are in areas of higher elevation

where the ground surface is higher above the groundwater table. Therefore, visually the datasets do indicate that there is some correlation between liquefaction damage and the non-liquefying crust thickness.

11. The non-liquefying crust thickness has been correlated with the *damage attribute* datasets. Even though there is a lot of scatter, the likelihood of liquefaction related damage increases with decreasing crust thickness. The scatter is attributed to other variables that control land performance. LPI, S and LSN consider some of these variables.
12. LPI produces correlations that show clear trends within each earthquake dataset, but vary between earthquakes (refer Figures G10 to G13). This limits the usefulness of LPI as a predictive tool as the ranges indicating damage vary depending on the magnitude and location of the earthquakes that may occur. The range of calculated LPI values is not consistent with the published indications of damage category.
13. There is no apparent relationship between the calculated settlement indicator S and the measured liquefaction induced ground settlement. The reasons for this include
 - a. Ejection of liquefied material
 - b. Lateral spread
 - c. Repeated liquefaction

However, there is a correlation between the calculated settlement indicator and the liquefaction and lateral spread observations (Figures G4 to G9). Therefore, the calculated settlement can be considered as a proxy for predicting the likelihood of liquefaction related damage. While calculated settlement shows a clear trend of differentiating the TC2, TC3 and residential Red Zone properties, there is a significant amount of overlap in properties that are less damaged and more severely damaged.

14. The LSN parameter refines the settlement parameter by including a depth weighting function. The depth weighting function recognises the importance of the non-liquefying crust thickness that ground surface damage from shallow liquefied layers is more likely than from deeper layers.
15. The LSN analyses show that there is a consistent correlation, both within each earthquake and between various earthquakes for the different categories of liquefaction and lateral spreading observations. The LSN clearly differentiates the most severely damaged land from the least severely damaged (Figures J1-J3). There is scatter in the data that is attributed to contributions from:
 - a. Inferences of geological conditions between CPT locations
 - b. Inferences on the spatial distribution of seismic loading
 - c. The inferences associated with the groundwater model
 - d. The quality of the crust
 - e. The probabilistic nature of liquefaction triggering
 - f. Whether the onset of liquefaction affects the soil profile response
 - g. Lateral spreading
 - h. The assumptions made to implement liquefaction triggering analyses on a regional basis
16. The analysis of the datasets indicates that there are clear correlations between LSN and adverse liquefaction effects. The LSN represents the risk of adverse liquefaction related damage occurring at the ground surface. Sites with high LSN are more likely to experience adverse effects than sites with low LSN. The LSN describes a range of possible site response (i.e. it is a probabilistic measure indicating risk).
17. LPI and LSN respond differently to changes in the PGA at sites. LPI is calculated as a direct function of the calculated FoS and so has a linear relationship with PGA. LSN and S use a correlation to densification strain and so have a smooth start and natural plateau with a 'S' shaped curve responding to PGA. LSN has a hyperbolic depth weighting function while

- LPI weights the liquefaction effects linearly. LSN is therefore significantly more sensitive to changes in non-liquefying crust thickness than LPI.
18. Of the three *calculated parameters* considered, LSN provides the best correlations with the liquefaction and lateral spreading observations and is the most suitable parameter for predicting future land performance in Canterbury. LSN also has moderately weak correlations with observed foundation damage.
 19. LSN is a good indicator of liquefaction vulnerability for residential land that is flat and confined. LSN is not intended to be an indicator of vulnerability to lateral spreading hazard and this is demonstrated by a case study in the Avonside area. Therefore, in order to identify land that is prone to liquefaction related ground surface deformation, the lateral spreading hazard areas need to be superimposed on areas with high potential LSN values.
 20. Photographs showing the response of sites with different calculated LSN are presented to demonstrate the typical range of behaviours for various LSN.
 21. The prediction of liquefaction damage from potential future earthquakes shows that land in the residential Red Zone is vulnerable at low levels of seismic load (i.e. under short return period earthquakes) and has the greatest vulnerability at higher levels of seismic load. Land in TC2 and TC3 areas is considerably less vulnerable than residential Red Zone land.

16 Acknowledgements

We acknowledge and recognise the significant contribution made to the report by many people at Tonkin & Taylor, in particular Virginie Lacrosse, James Lyth, Joseph Simpson, Andy Huang, Mike Jacka, Hannah Udell, John Leeves, Mark Broadbent and Christopher Pedrezuela. Simon Cox (GNS) and Hugh Cowan (EQC) have provided ongoing support during the work relating to this report and we thank them for this. The discussions, comments and insightful review of Prof Tom O'Rourke, Prof Jon Bray and Prof Misko Cubrinovsky are gratefully acknowledged.

This work would not have been possible without the contribution of the New Zealand Government through its agencies the Earthquake Commission, Canterbury Earthquake Recovery Authority, Ministry of Civil Defence and Emergency Management and Land Information New Zealand. The data collected, processed and supplied by these agencies has enabled this study to be undertaken in a supportive and collegial manner, and their assistance is appreciated.

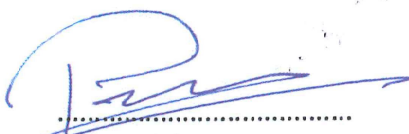
Tonkin & Taylor LTD

Environmental and Engineering Consultants

Report prepared by:

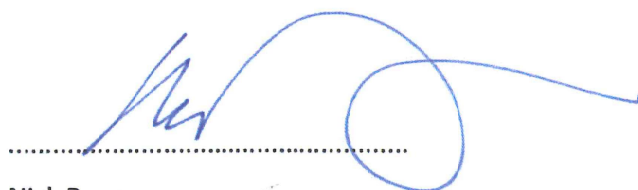


Sjoerd van Ballegooy
Project Manager



Pierre Malan
Senior Geotechnical Engineer

Authorised for Tonkin & Taylor Ltd by:



Nick Rogers
Project Director

PMM
Liquefaction Vulnerability Study version FB February 2013

References

- Beavan, R.J., Samsonov, S., Motagh, M., Wallace, L.M., Ellis, S.M., Palmer, N.G., (2010) *The Darfield (Canterbury) earthquake: geodetic observations and preliminary source model* Bulletin of the New Zealand Society for Earthquake Engineering 43(4): 228-235.
- Beavan, R.J., Fielding, E.J., Motagh, M., Samsonov, S., Donnelly, N., (2011) *Fault location and slip distribution of the 22 February 2011 Mw 6.2 Christchurch, New Zealand, earthquake from geodetic data* Seismological Research Letters 82(6): 789-799.
- Beavan, R.J., Motagh, M., Fielding, E.J., Donnelly, N., Collett, D. (2012) *Fault slip models of the 2010-2011 Canterbury, New Zealand, earthquakes from geodetic data and observations of postseismic ground deformation* New Zealand Journal of Geology and Geophysics 55(3): 207-221.
- Berryman, K. (2012) Pers. Comm. *Magnitudes of earthquakes in June and December 2011*
- Bouckovalas, G. & Dakoulas, P. (2007) *Liquefaction performance of shallow foundation in presence of a soil crust*, Earthquake Geotechnical Engineering, Chapter 11, 245-276
- Bradley B. A. (2012a) *A critical analysis of strong ground motions observed in the 4 September 2010 Darfield*. Soil Dynamics and Earthquake Engineering; (submitted for publication)
- Bradley and Hughes (2012b) *Conditional Peak Ground Accelerations in the Canterbury Earthquakes for Conventional Liquefaction Assessment*, Technical Report for the Ministry of Business, Innovation and Employment, April 2012. 22p.
- Bradley and Hughes (2012c) *Conditional Peak Ground Accelerations in the Canterbury Earthquakes for Conventional Liquefaction Assessment: Part 2*, Technical Report for the Ministry of Business, Innovation and Employment, December 2012. 19p.
- Bray J.D. & Sancio, R.B (2006) *Assessment of the liquefaction susceptibility of fine grained soils* ASCE Journal of Geotechnical and Geoenvironmental Engineering, Vol. 132(9), 1165-1177
- Canterbury Earthquake Recovery Authority (CERA) (2012) *Canterbury Land Information Map Kaiapoi Lakes to Governors Bay 23rd March 2012*
- Cascone, E. & Bouckovalas, G (1998) *Seismic bearing capacity of footings on saturated sand with a clay cap* 11th European Conference on Earthquake Engineering, 1998. Balkema, Rotterdam, ISBN 90 5410 982 3
- Idriss, I.M. & Boulanger, R.W. (2008). *Soil liquefaction during earthquakes*, MNO-12, Earthquake Engineering Research Institute, 242p
- Ishihara, K. (1985). *Stability of Natural Deposits During Earthquakes* Proceedings of the 11th International Conference on Soil Mechanics and Foundation Engineering, San Francisco, 1:321-376
- Iwasaki, T., Arakawa, T. & Tokida, K. (1982). *Simplified Procedures for Assessing Soil Liquefaction During Earthquakes* Proc. Conference on Soil Dynamics and Earthquake Engineering. Southampton, 925-939
- Iwasaki, T., Tatsuoka, F., Tokida, K.-i., and Yasuda, S., (1978). *A practical method for assessing soil liquefaction potential based on case studies at various sites in Japan*, in Proceedings, 2nd International Conference on Microzonation, San Francisco, pp. 885-896.

- Juang, C.H, Yang, S.H, Yuan, H., Fang, S.Y. (2005) *Liquefaction in the Chi-Chi earthquake – effect of fines and capping non-liquefiable layers* Journal of the Japanese Geotechnical Society of Soils and Foundations, Vol. 45 No. 6 pp 89-101
- Milashuk, M. (2012) *Acceleration records from selected aftershocks*, pers.comm
- Ministry of Business, Innovation & Employment (2012). *Revised issue of Repairing and rebuilding houses affected by the Canterbury earthquakes*, December 2012
- Moss, R. E. S., Seed, R. B., Kayen, R. E., Stewart, J. P., Kiureghian, A. D., & Cetin, K. O., (2006). *CPT-based probabilistic and deterministic assessment of in situ seismic soil liquefaction potential*, ASCE Journal of Geotechnical and Geoenvironmental Engineering, Vol. 132(8), 1032-1051,
- O'Rourke, T. & Milashuk, S. (2012). Personal communication to T&T, contours of peak ground accelerations for September 2010, February, June and December 2011 earthquakes
- Robertson, P.K. & Cabal, K.L., (2010). *Estimating soil unit weight from CPT*, 2nd International Symposium on Cone Penetration Testing, Huntington Beach, California
- Robertson, P.K. & Wride, C.E., (1998). *Evaluating cyclic liquefaction potential using the cone penetration test*, Canadian Geotechnical Journal, 35:442 – 459
- Seed, H.B. & Idriss, I.M. (1971). *Simplified procedure for evaluating soil liquefaction potential*: Proceeding of the American Society of Civil Engineers, Journal of the Soil Mechanics and Foundations Division, v. 93, no. SM9, 1249-1273
- Weeber, J.H., (2008) *Christchurch groundwater protection: a hydrogeological basis for zone boundaries, Variation 6 to the Proposed Natural Resources Regional Plan Environment Canterbury*, Report no. U08/21 ISBN 978-1-86937-802-8 60p.
- van Ballegooy, S., Cox, S. C., Agnihotri, R., Reynolds, T., Thurlow, C., Rutter, H. K., Scott, D.M. Begg, J. G., McCahon, I. (2013) *Median water table elevation in Christchurch and surrounding area after the 4 September 2010 Darfield Earthquake*. GNS Science Report 2013/01 (in final draft at time of issue)
- Youd, T.L. & Garris, C.T. (1995). *Liquefaction-induced ground surface disruption* ASCE Journal of Geotechnical Engineering 121 (11), 805 – 809
- Zhang, G., Robertson, P. K., & Brachman, R. W. I. (2002). *Estimating liquefaction-induced ground settlements from CPT for level ground*, Canadian Geotechnical Journal, 39, 1168–80



Tonkin & Taylor

ENVIRONMENTAL AND ENGINEERING CONSULTANTS

